JCI The Journal of Clinical Investigation

MAP kinase phosphatase-1 inhibition of p38α within lung myofibroblasts is essential for spontaneous fibrosis resolution

Sean M. Fortier, … , Anton M. Bennett, Marc Peters-Golden

J Clin Invest. 2024. https://doi.org/10.1172/JCI172826.

Research In-Press Preview Cell biology Pulmonology

Graphical abstract

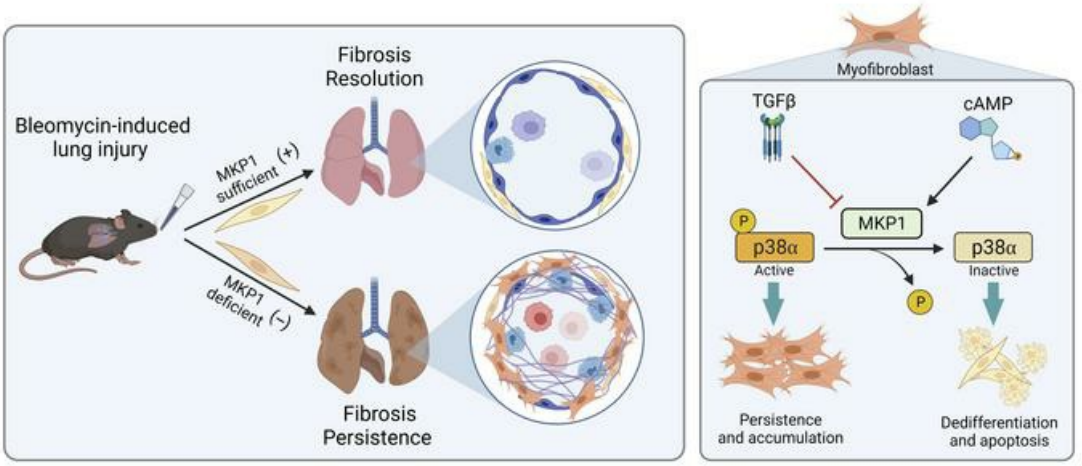

MAP kinase phosphatase-1 inhibition of p38α within lung myofibroblasts is essential for spontaneous fibrosis resolution

Sean M. Fortier[1], Natalie Walker[1], Loka R. Penke[1], Jared Baas[1], Qinxue Shen[1,2], Jennifer Speth[1], Steven K. Huang[1], Rachel L. Zemans[1], Anton M. Bennett[3] , Marc Peters-Golden[1]*

[1]Division of Pulmonary and Critical Care Medicine, University of Michigan Medical School, Ann Arbor, MI 48109, [2]Department of Pulmonary and Critical Care Medicine, The Second Xiangya Hospital, Central South University, Changsha, Hunan 410011, China, and [3]Department of Pharmacology, Yale University School of Medicine, New Haven, CT 06520.

Loka R. Penke current affiliation: Ionis Pharmaceuticals, Inc. 2855 Gazelle Court Carlsbad, CA 92010.

*Corresponding Author

Marc Peters-Golden, M.D.

6301 MSRB III

1150 W. Medical Center Drive

Ann Arbor, MI 48109-5642, USA

Email: petersm@umich.edu

Phone: 734-936-5047

Fax: 734-764-4556

The authors have declared that no conflict of interest exists.

Abstract

Fibrosis following tissue injury is distinguished from normal repair by the accumulation of pathogenic and apoptosis-resistant myofibroblasts (MFs), which arise primarily by differentiation from resident fibroblasts. Endogenous molecular brakes that promote MF dedifferentiation and clearance during spontaneous resolution of experimental lung fibrosis may provide insights that could inform and improve treatment of progressive pulmonary fibrosis in patients. MAP kinase phosphatase-1 (MKP1) influences cellular phenotype and fate through precise and timely regulation of MAPK activity within various cell types and tissues, yet its role in lung fibroblasts and pulmonary fibrosis has not been explored. Utilizing gain- and loss-of-function studies, we found that MKP1 promoted lung MF dedifferentiation and restored their sensitivity to apoptosis – effects determined to be mainly dependent upon its dephosphorylation of p38α MAPK (p38α). Fibroblast-specific deletion of MKP1 following peak bleomycin-induced lung fibrosis largely abrogated its subsequent spontaneous resolution. Such resolution was restored by treating these transgenic mice with the p38α inhibitor VX-702. We conclude that MKP1 is a critical antifibrotic brake whose inhibition of pathogenic p38α in lung fibroblasts is necessary for fibrosis resolution following lung injury.

Introduction

Fibrosis is a disordered response to tissue injury characterized by abnormal wound healing and organ scarring. In pulmonary fibrosis, collagen accumulation and contraction of the parenchyma distort lung architecture and interfere with gas exchange. The prototypic fibrotic lung disease – idiopathic pulmonary fibrosis (IPF) – is a common and severe disorder typically progressing to respiratory failure and death within 3 – 5 years (1, 2). The ultimate effector cell in IPF is the myofibroblast (MF) – a distinct mesenchymal cell derived from the differentiation of resident lung fibroblasts that contributes to lung scarring and stiffness through secretion of collagens and matrix proteins and expression of contractile stress fibers and focal adhesions, respectively (3, 4).

Because patients with IPF invariably manifest established scarring at the time of clinical presentation, a truly impactful treatment strategy must not only prevent progression but also reverse existing fibrosis. A key feature of MFs that enables fibrosis to endure and progress in IPF and other fibrotic disorders is their resistance to apoptosis and subsequent accumulation (5, 6) – in glaring contrast with their timely clearance during normal wound healing (7, 8). Indeed, it has been demonstrated that spontaneous fibrosis resolution – a characteristic and in some respects problematic feature of the bleomycin mouse model of pulmonary fibrosis – requires Fas-mediated lung MF apoptosis (16). Though once considered irreversible, it is now well-recognized that in vitro dedifferentiation of the MF phenotype can proceed via a variety of molecular pathways (9-14). Importantly, some but not all of these pathways concomitantly restore MF sensitivity to apoptosis (15). However, the endogenous molecular mediators and

signaling pathways that promote MF dedifferentiation and enable their apoptosis – thus recapitulating normal wound healing and potentially enabling fibrosis resolution following lung injury – remain unknown. Furthermore, the capacity of the two currently approved pharmacotherapies for IPF, pirfenidone and nintedanib, to dedifferentiate established MFs has not been explored.

The MAPKs comprise three families of constitutively expressed proteins – p38 MAPK (p38), JNK, and ERK – that are known to influence numerous biological processes including fibroblast differentiation, survival, and proliferation (16-18). Precise spatiotemporal regulation of MAPKs is crucial and requires their post-translational phosphorylation/dephosphorylation (19, 20). Profibrotic stimuli, such as TGFβ-1 (TGFβ), and fibrotic states are associated with increased levels of activated p38, JNK, and ERK within lung fibroblasts (21-24). However, the influence of these MAPKs on MF plasticity and thus their potential role in maintaining persistent fibrosis is not known (25).

The MAPK phosphatases (MKPs, also known by their gene category name dual specificity phosphatases or DUSPs) dephosphorylate the regulatory tyrosine and threonine residues of MAPKs and thus function as a key brake on their activity (26, 27). MKP1 (encoded by *DUSP1*) is one of 10 catalytically active MKPs expressed in mammalian cells and belongs to the "inducible nuclear" subclass (26). Following mitogen- or stress-induced stimuli, MKP1 is rapidly upregulated and localizes to the nucleus where it is known to regulate cell phenotypes in several tissues, including skeletal/cardiac muscle, liver, bone, and brain (28-32). We have previously linked the antifibrotic actions of the drug bortezomib to its ability to induce

expression of MKP1 (but not other MKP proteins) in lung fibroblasts (33). However, the specific effect of MKP1 on MF phenotype, its downstream MAPK effector targets, and its role as an endogenous brake on pulmonary fibrosis remains unexplored.

In the present study, we utilize in vitro lentiviral transduction techniques to generate inducible MKP1-overexpressing and CRISPR/Cas9-mediated MKP1-deficient human lung fibroblasts (HLFs), and demonstrate that MKP1 inhibition of p38α, but not JNK or ERK, leads to MF dedifferentiation in vitro and restored sensitivity to apoptosis. Moreover, Cre recombinase-mediated deletion of *Dusp1* in mouse fibroblasts initiated following peak bleomycin-induced pulmonary fibrosis abrogates spontaneous resolution in vivo*,* indicating that MKP1 serves as a critical antifibrotic brake promoting fibrosis resolution. Indeed, fibrosis resolution was restored in mouse lungs whose fibroblasts lack MKP1 following administration of a p38α-specific inhibitor.

Results

MKP1 (*DUSP1*) is the chief DUSP isoform expressed in normal lung fibroblasts, is reduced in IPF fibroblasts, and is downregulated by TGFβ.

Using the Chan Zuckerberg Initiative online database (https://cellxgene.cziscience.com/), we determined the relative prevalence and levels of expression of transcripts encoding each of the catalytically active DUSP proteins among available human and mouse lung fibroblast subtypes (Figure 1A). *DUSP1* was the most commonly expressed and abundant isoform measured in fibroblasts of normal lungs from both human and mouse, and its expression was also noted in several other cell types (Supplemental Figure 1A and B). Analysis of publicly available single cell RNA sequencing data (http://www.ipfcellatlas.com/) did not reveal substantial differences in MKP1 transcript levels in any fibroblast subtype between normal lungs and those afflicted with IPF or interstitial lung disease (Supplemental Figure 1C and D). However, we found that MKP1 protein expression in IPF fibroblasts was reduced when compared to that in normal HLFs (Figure 1B), suggesting possible differences in post-transcriptional regulation of MKP1 in IPF versus normal HLFs. In keeping with this observation, treatment of normal HLFs with the pivotal profibrotic mediator TGFβ reduced MKP1 protein and mRNA concomitant with an increase in collagen 1A1 (Col1A1) protein (Figure 1C). However, this effect was transient, demonstrating a nadir at 3 h following TGFβ treatment with return of transcript and protein expression to baseline at 24 h (Supplemental Figure 1E and F). Such rapid and labile modulation of MKP1 expression is consistent with the strict temporal regulation of MKPs in other cell types (34-36). These data

thus demonstrate that lung fibroblast MKP1 protein expression is reduced in cells from patients with pulmonary fibrosis and in those exposed to a fibrotic stimulus well known to be abundant in fibrotic lungs (37).

MKP1 deletion in lung fibroblasts potentiates collagen production while its overexpression leads to myofibroblast dedifferentiation and restored sensitivity to apoptosis.

To evaluate the role of baseline MKP1 expression on canonical fibrosis-associated gene expression in vitro, normal HLFs were infected with lentivirus containing a lentiCRISPR plasmid (TLCV2) with a constitutively expressed sgRNA targeting *DUSP1/*MKP1 (or a non-targeting sgRNA control) and a doxycycline-inducible Cas9. After pretreatment for 48 h with doxycycline, fibroblasts were treated with TGFβ to promote MF differentiation. Doxycycline treatment efficiently reduced MKP1 expression, leading to an increase in TGFβ-induced expression of Col1A1, fibronectin (FN1), and the fibroblast activation-associated gene CTHRC1 without a significant change in αSMA protein (Figure 2A). MKP1-deficient HLFs also exhibited reduced caspase 3/7 activity following exposure to an anti-Fas activating antibody (Supplemental Figure 2B). Based on these data showing that MKP1 negatively fibroblast activation and reduces their sensitivity to apoptosis, we reasoned that its overexpression might promote MF dedifferentiation and restore apoptosis sensitivity in these cells. To test this hypothesis, we transduced normal HLFs with lentivirus containing an inducible MKP1 (or GFP) overexpression construct, treated these cells with TGFβ to generate MFs, and subsequently induced MKP1 overexpression with doxycycline. As expected, there was a substantial increase in MKP1

transcript at 24 h following doxycycline treatment (Supplemental Figure 2A). MKP1 protein expression in these MFs was also markedly increased and associated with a reduction in αSMA, Col1A1, FN1, and CTHRC1 protein and RNA expression (Figure 2B, Supplemental Figure 2A). Organized αSMA stress fiber content – as indicated by immunofluorescent staining – was likewise reduced in MFs overexpressing MKP1 (Figure 2C). Similarly, MKP1 overexpression in otherwise untreated IPF fibroblasts led to a reduction in αSMA, Col1A1, and FN1 protein without a change in CTHRC1 expression (Figure 2D). Crucially, MKP1 overexpression increased Fas-induced caspase 3/7 activity and annexin V membrane expression (Figure 2E), indicating that MKP1 upregulation restores apoptosis sensitivity in MFs in vitro. These results demonstrate that MKP1 can dedifferentiate MFs toward an apoptosis-sensitive phenotype.

Lung fibroblast expression of MKP1 mitigates peak fibrosis and is essential for spontaneous fibrosis resolution following in vivo administration of bleomycin.

As MKP1 serves as an antifibrotic brake in vitro by promoting MF dedifferentiation and restoring Fas-mediated apoptosis, we hypothesized that its constitutive expression in lung fibroblasts mitigates the severity of peak fibrosis and is necessary for spontaneous fibrosis resolution following lung injury in vivo. To address these hypotheses, we utilized a previously reported C57BL/6 transgenic mouse strain with *loxP* regions spanning exons 2 and 3 of *Dusp1* (38) and crossed it with C57BL/6 mice containing an inducible fibroblast-specific Cre (39). The resulting $Col1a2^{CreERT2}$;$Dusp1^{fl/fl}$ mice (or their Cre negative littermate controls) were treated

with tamoxifen at the indicated times following bleomycin-induced lung injury to specifically delete MKP1 in fibroblasts.

To assess the role of MKP1 in lung fibroblasts during fibrogenesis, *Col1a2*^{CreERT2};*Dusp1*$^{fl/fl}$ and *Dusp1*$^{fl/fl}$ mouse lungs were instilled with bleomycin (1.0 U/kg) by oropharyngeal (o.p.) administration (day 0), followed by introduction of a tamoxifen chow diet starting on day 9, with sacrifice and lung harvest on day 21 (Figure 3A). The time frame of days 9-21 was chosen to reflect the post-inflammatory fibrotic phase in this model. Tamoxifen successfully promoted *loxP* recombination of the *Dusp1*$^{fl/fl}$ locus (Figure 3B, left) resulting in a near complete elimination of MKP1 protein (Figure 3B, right) in Cre positive mice compared to Cre negative controls. As expected, bleomycin induced an approximate doubling of hydroxyproline content in Cre negative mouse lungs at day 21 (Figure 3C). Consistent with our in vitro finding that MKP1 deletion in MFs promoted higher collagen I expression (Figure 2A), bleomycin-treated lungs from Cre positive mice demonstrated a significantly greater hydroxyproline content than Cre negative mice (Figure 3C). Histopathologic analysis using Masson's trichrome staining of collagens (Figure 3D) further indicated an increase in severity of pulmonary fibrosis in Cre positive mice.

Pulmonary fibrosis arising from single-dose intrapulmonary bleomycin is well known to eventually resolve spontaneously in the lungs of young mice (40-42). Although this has often been viewed as a limitation to the model, it provides a unique opportunity to identify and study endogenous antifibrotic brakes whose deletion might abrogate such spontaneous resolution. We therefore sought to determine the role of lung fibroblast MKP1 during the resolution phase

of bleomycin-induced pulmonary fibrosis. To specifically assess MKP1 during resolution, tamoxifen chow was provided to *Col1a2*^{CreERT2};*Dusp1*$^{fl/fl}$ and *Dusp1*$^{fl/fl}$ mice following the establishment of bleomycin-induced peak fibrosis (at day 21) and maintained until sacrifice on day 42 or 63 (Figure 3E). As expected, and as measured by hydroxyproline quantitation of lung collagen content, Cre negative mice demonstrated partial fibrosis resolution at day 42 and near complete resolution by day 63 (Figure 3G). By contrast, Cre positive mice failed to exhibit any decrease in lung collagen content by days 42 or 63, indicating a failure of spontaneous fibrosis resolution (Figure 3G). Failure of spontaneous resolution was also demonstrated by histopathology in Cre positive mice at days 42 and 63 (Figure 3F). We performed immunofluorescence microscopy of lung sections from mice harvested at each time point to assess the kinetics of MKP1 and αSMA expression during resolution. Similar to the transient TGFβ-mediated reduction of MKP1 in vitro, we found MKP1 expression to be markedly reduced in αSMA+ MFs in lung sections obtained from Cre negative mice at peak fibrosis but was restored in αSMA+ MFs in lung sections from these mice at day 42 (Supplemental Figure 3A). Notably, αSMA expression was far less abundant and stress fibers appeared to be disorganized in fibroblasts expressing MKP1 in Cre negative mice at day 42 and 63, consistent with MF clearance and dedifferentiation, respectively. Moreover, αSMA+ MFs from Cre negative day 42 lung sections displayed positive TUNEL staining indicating apoptosis-mediated clearance (Supplemental Figure 3B). Consistent with our hydroxyproline and histopathologic data, and in contrast to the findings noted above in Cre negative mice, αSMA+ MFs remained abundant in lung sections from Cre positive mice at days 42 and 63.

Whole lung mRNA expression of the fibrosis-associated genes *Fn1*, *Tgfb1, Cthrc1,* (43), *Col3a1* and anti-apoptotic *Birc5* was increased in the lung homogenates of Cre positive mice sacrificed on day 42 compared to Cre negative mice (Supplemental Figure 4A), a finding consistent with the non-resolving nature of fibrosis in mouse lungs whose fibroblasts lack MKP1. We also measured genes from whole lung lysates specifically associated with fibroblast subtypes (44). Lipofibroblasts were identified by *Plin2*, fibrosis-injury associated fibroblasts by *Pdgfrb*, and distinct subsets of matrix fibroblasts by *Col13a1* or *Col14a1* (Supplemental Figure 4B). With the exception of *Col14a1*, each transcript was markedly upregulated at peak fibrosis. Moreover, *Col13a1* and *Pdgfrb* expression declined slower in Cre positive mouse lungs, and remained significantly higher at day 42 than in those from Cre negative mice. Interestingly, transcripts of each gene in Cre positive mice were reduced by day 63 to the levels measured in Cre negative mouse lungs despite the persistence of fibrosis demonstrated by lung hydroxyproline content (Figure 3G) and histopathology (Figure 3F). Therefore, whole lung mRNA levels of fibrosis-associated genes measured on day 42 better reflect global indices of persistent fibrosis/resolution than their levels determined on day 63, perhaps because day 42 represents a more dynamic point of the resolution response. Together, these data indicate both that MKP1 within fibroblasts acts as a brake on peak lung fibrosis and is necessary for spontaneous fibrosis resolution.

Cellular crosstalk among mesenchymal, epithelial, and immune cells is an important aspect of tissue repair and homeostasis. We thus assessed the effect of MKP1 deletion within lung fibroblasts on epithelial cells and macrophages by performing immunofluorescence microscopy at partial resolution (day 42). Lung sections from Cre negative mice displayed

typical ratios of type I (PDPN+) and type II (proSPC+) alveolar epithelial cells consistent with their grossly normal alveolar structure, while Cre positive lung sections displayed regions largely devoid of type I cells (Figure 3H). Additionally, abnormal regions of parenchymal bronchiolization (E-cadherin+ subpleural tubular structures) were present in Cre positive lung sections but completely absent in Cre negative lungs (Figure 3I). Likewise, substantially higher numbers of alveolar macrophages (CD68+ cells) were present in Cre positive mouse lungs compared to Cre negative controls, indicative of persistent inflammation (Figure 3J). A similar pattern displaying patchy regions lacking type I epithelial cells associated with macrophage infiltration was demonstrated in lung sections from mice harvested at peak fibrosis (Supplemental Figure 3C). These data demonstrate that the impaired resolution observed in mice lacking MKP1 within the fibroblast compartment is characterized not only by accumulation of activated MFs, but also by dysregulation of epithelial and macrophage populations.

p38 is the MAPK whose inhibition by MKP1 accounts for its ability to dedifferentiate myofibroblasts.

MKP1 is known to target all three MAPK families – p38, JNK, and ERK (26, 45, 46) – but cellular context and post-translational modifications greatly influence the degree to which MKP1 interacts with or inhibits each (47, 48). To determine the kinase(s) whose inhibitory targeting is responsible for the ability of MKP1 to promote lung MF dedifferentiation, we assessed its ability to dephosphorylate each MAPK in vitro. Utilizing the same MKP1

overexpression strategy as detailed in Figure 2B, we demonstrated that MKP1 promotes dephosphorylation of p-p38 (using a Thr180/Tyr182-specific antibody), but not of p-ERK or p-JNK, in TGFβ-elicited lung MFs (Figure 4A). This effect of MKP1 overexpression on p-p38 was also demonstrated in IPF fibroblasts (Supplemental Figure 5A). In a complementary approach, Cas9-mediated deletion of MKP1 led to an increase in p-p38 with no change in p-ERK and p-JNK (Figure 4B). Additionally, immunohistochemical staining for p-p38 in mouse lung sections demonstrated greater staining within fibrotic regions in Cre positive mice (fibroblast-specific MKP1 null) than in Cre negative nice (WT fibroblast MKP1 expression) (Supplemental Figure 5B). To further correlate p-p38 levels with MKP1 over time, normal patient-derived HLFs were treated with TGFβ to activate p38. The TGFβ-mediated increase in p-p38 over 24 h significantly correlated with a relative decline in MKP1 with a Pearson co-efficient of r = -0.64 (Supplemental Figure 5C). Taken together, these data therefore suggest that p38 is the major MAPK directly inhibited by MKP1 in lung MFs within this experimental context.

We next employed a distinct experimental strategy to evaluate if pharmacologic p38 inhibition dedifferentiates lung MFs. Indeed, treatment of MFs with the commonly employed p38 inhibitor SB203580 (49) reduced expression of αSMA and Col1A1 proteins (Figure 4C) and transcripts (Supplemental Figure 5D) as well as αSMA organization into stress fibers (Figure 4D). p38 inhibition with SB203580 also restored Fas-mediated apoptosis sensitivity in lung MFs (Figure 4E). These data implicate p38 inactivation as the mechanism by which MKP1 promotes MF dedifferentiation and clearance.

p38α is the isoform whose inhibition by MKP1 promotes myofibroblast dedifferentiation.

There are four p38 isoforms in the mammalian genome – α, β, ɣ, and δ (50) – with relative expression of each dependent upon tissue and cell type. The alpha and beta isoforms are ubiquitously expressed while gamma and delta expression are tissue-restricted (51). Moreover, p38α and β are readily dephosphorylated by several MKP proteins while ɣ and δ are resistant to all known MKPs (52, 53). We thus measured p38α and β transcript levels by qPCR in normal HLFs, TGFβ-elicited MFs, and in IPF fibroblasts (Figure 5A). Each expressed substantially higher (~20 fold) p38α transcript levels compared to p38β. To determine whether p38α protein expression was indeed the most highly translated isoform, we measured the reduction in total p38 protein following CRISPR/Cas9-mediated deletion of *MAPK14* (p38α). This inducible CRISPR/Cas9 line was generated using the same TLCV2 plasmid and method used to delete *DUSP1* (Figure 2A). Following successful deletion of p38α (Figure 5B, left), we quantified the relative proportion of total p38 attributable to p38α by subtracting the densitometric value of the total p38 band in fibroblasts containing the *MAPK14* sgRNA from that of the total p38 band in the control (Figure 5B, right). Quantification using this approach revealed that p38α accounts for ~50% of the total p38 protein expressed in lung MFs. Further analysis using a sgRNA targeting *MAPK12* revealed that p38ɣ accounted for the vast majority of remaining p38 mRNA and protein (Supplemental Figure 6A and B), thus suggesting that p38α (as opposed to β) is the predominant target of MKP1 in lung fibroblasts.

To determine if p38α is indeed the downstream isoform target of MKP1 whose inhibition is responsible for lung MF dedifferentiation, we utilized the aforementioned inducible

p38α CRISPR line. Fibroblasts transduced with lentiCRISPR constructs expressing a *MAPK14*-targeting sgRNA were treated with TGFβ for 48 h to establish MFs. Dedifferentiation was then assessed following doxycycline-induced Cas9 expression for 96 h. Deletion of p38α promoted MF dedifferentiation, as demonstrated by the substantial reduction in αSMA and Col1A1 protein (Figure 5C).

To further confirm the influence of p38α in lung MFs, we employed a pharmacologic approach utilizing its isoform-specific inhibitor VX-702 (54). We found that elicited MFs treated with VX-702 indeed exhibited significantly reduced αSMA and Col1A1 proteins (Figure 5D) and transcripts (Supplemental Figure 6C), and promoted efficient disassembly of αSMA stress fibers by immunofluorescent microscopy (Figure 5E). Moreover, MFs dedifferentiated with VX-702 demonstrated restoration of apoptosis sensitivity as indicated by upregulation of cleaved caspase 3/7 and annexin V (Figure 5F). Similar effects of dedifferentiation and apoptosis were observed in IPF fibroblasts treated with VX-702 independent of MKP1 levels (Supplemental Figures 6D, E, and F). These complementary data with both knockdown and pharmacologic inhibition indicate that p38α is the likely downstream target of MKP1 whose inhibition is sufficient to dedifferentiate lung MFs and restore their sensitivity to apoptosis.

The p38α-specific inhibitor VX-702 mitigates bleomycin induced fibrosis and restores spontaneous fibrosis resolution in mice with MKP1-deficient fibroblasts.

Having identified a crucial role of p38α as a determinant of the pathogenic MF phenotype in vitro and its robust inhibition by VX-702, we next evaluated the in vivo impact of

pharmacologic p38α inhibition during fibrogenesis. Specifically, C57BL/6 male and female mice were treated daily with VX-702 (10 mg/kg) by oral gavage (o.g.) starting on day 9 following bleomycin (1.0 U/kg o.p.) until sacrifice and lung harvest on day 21 (Figure 6A). Bleomycin-treated mice that received VX-702 exhibited less total lung collagen by hydroxyproline content compared to bleomycin-treated controls (Figure 6B). Similarly, peak fibrosis was less severe by histopathology among VX-702-treated mice compared to those treated with bleomycin alone (Figure 6C).

We next sought to test the hypothesis that p38α is a key driver of persistent fibrosis and that its inhibition by MKP1 following peak fibrosis promotes spontaneous fibrosis resolution. The same *Col1a2*^{CreERT2};*Dusp1*$^{fl/fl}$ mice utilized in the previous in vivo studies (Figure 3) were treated with bleomycin (1.0 U/kg) followed at day 21 by introduction of a tamoxifen diet and daily treatment with VX-702 or vehicle by o.g. (Figure 6D). Mice were sacrificed on day 56 for lung harvest – a time point at which fibrosis resolution is substantial and similar to that observed at day 63 (data not shown). Consistent with the data displayed in Figure 3, Cre positive *Dusp1*$^{fl/fl}$ mice treated with vehicle exhibited substantially higher hydroxyproline content than Cre negative controls, indicating impaired resolution (Figure 6E). Importantly, VX-702 treatment in these Cre positive mice reduced hydroxyproline content nearly to the level of Cre negative mice exhibiting spontaneous fibrosis resolution (Figure 6E). Histopathology further demonstrated spontaneously resolving fibrosis among Cre negative mice, persistent fibrosis in the Cre positive cohort, and reversal of persistent fibrosis in Cre positive mice treated with VX-702 (Figure 6F). Whole lung RNA measured in lung homogenates of vehicle-treated Cre positive mice at day 56 demonstrated elevated levels of the fibrosis-associated genes *Fn1*, *Tgfb1*, *Acta2*,

Col1a1, and *Col3a1* as well as elevation of the pro-survival gene *Birc5* and a trend favoring elevation of the pathologic fibroblast marker *Cthrc1*. Remarkably, lung homogenates from Cre positive mice treated with VX-702 displayed significant reduction in the expression of each of these genes to levels seen in Cre negative mice (Figure 6G). Transcript markers of fibroblast subsets were measured in whole lung lysates from each condition (Supplemental Figure 7B). Again, *Col13a1* demonstrated elevation in Cre positive mice, but *Col14a1*, *Plin2*, and *Pdgfrb* were not significantly different at this time point. Inhibition of p38α via VX-702 significantly reduced matrix fibroblast markers *Col13a1* and *Col14a1*. These in vivo data combining pharmacologic treatment of fibroblast-specific knockout mice strongly implicate p38α as the fibrotic driver whose inhibition by MKP1 within lung fibroblasts promotes spontaneous fibrosis resolution.

MKP1 induction is essential for PGE_2/cAMP/PKA-mediated inhibition of p38 and myofibroblast dedifferentiation.

Our data suggest that MKP1 expression in lung MFs is necessary for spontaneous fibrosis resolution via p38α inhibition in vivo and for their dedifferentiation and clearance in vitro. Mediators and signaling events that might contribute to these pro-resolution phenomena are of obvious interest. cAMP signaling has been extensively investigated in this context and has been linked with a variety of antifibrotic effects (55). One such cAMP-dependent mediator is prostaglandin E_2 (PGE_2), which has been shown to be diminished in the lungs (56) and in lung fibroblasts of patients with IPF (57), and to directly promote both MF dedifferentiation (11) and

apoptosis (15, 58). PGE_2/cAMP have also been shown to induce MKP1 in a variety of cell types (59-61), but whether this is the case in lung fibroblasts and whether such induction participates in pro-resolution effects of PGE_2 in mesenchymal cells has not been explored. We therefore assessed the effects of PGE_2 and its canonical downstream cAMP effector molecules on MKP1 induction and p38 inhibition in lung MFs. MKP1 protein expression was rapidly upregulated by PGE_2, the direct adenylyl cyclase agonist forskolin, and the protein kinase A (PKA)-specific cAMP analog 6-BNZ-cAMP (Figure 7A). Importantly, MKP1 induction by each of these agonists was associated with p38 dephosphorylation. Conversely, the exchange protein activated by cAMP (Epac)-specific agonist 8-pCPT-cAMP did not affect MKP1 gene expression or modulate p38 phosphorylation. PGE_2-mediated induction of MKP1 with concomitant p38 dephosphorylation was confirmed in IPF fibroblasts (Supplemental Figure 8).

These results are consistent with our previously published findings that PGE_2 prevents TGFβ-induced p38 phosphorylation (21) and promotes lung MF dedifferentiation through the cAMP/PKA axis (11, 15), and point to a possible role for MKP1 as a downstream effector of this pathway in lung fibroblasts. To test this possibility, we again utilized a CRISPR/Cas9 approach to delete *DUSP1* in lung MFs followed by treatment with PGE_2. Treatment of control MFs with PGE_2 was associated with increased MKP1 expression and p38 dephosphorylation. By contrast, PGE_2 treatment did not promote substantial p38 dephosphorylation in MKP1 null MFs (Figure 7B, top). Using an independent approach, we isolated lung fibroblasts from *Col1a2*^{CreERT2}*;Dusp1*$^{fl/fl}$ and *Dusp1*$^{fl/fl}$ mice 10 days following introduction of a tamoxifen chow diet and treated these cells with TGFβ for 48 h to generate MFs. We then treated both WT and MKP1 null fibroblasts with PGE_2 (Figure 7B, bottom). Indeed, p38 phosphorylation was greatly

reduced in MKP1-expressing fibroblasts treated with PGE_2 but remained unchanged in MKP1 null mouse lung fibroblasts. Furthermore, MKP1 deletion largely abrogated the PGE_2-mediated reduction in αSMA protein and abolished its ability to reduce Col1A1 protein in human lung MFs (Figure 7C). These findings suggest that MKP1 is necessary for the ability of PGE_2/cAMP signaling to negatively regulate p38 activity and to dedifferentiate lung MFs.

The two FDA approved antifibrotic drugs pirfenidone and nintedanib fail to dephosphorylate p38 and to promote dedifferentiation of human lung myofibroblasts.

Although current FDA approved drugs pirfenidone and nintedanib slow the decline in lung function in patients with IPF, they notably fail to resolve established fibrosis (62, 63). Whether these agents elicit dedifferentiation of MFs that may underly fibrosis resolution is unknown. Moreover, their effects on p38 signaling in MFs remain incompletely characterized. Nintedanib might be expected to influence p38 activation through its established inhibition of the FGF, PDGF, and VEGF receptors that signal via MAPKs (64). Pirfenidone – whose mechanism of action is not fully characterized – has been shown to reduce TGFβ signaling (65) and inhibit p38ɣ (66). We tested the capacity of each of these FDA-approved drugs to prevent fibroblast-to-MF differentiation, promote MF dedifferentiation, and modulate p38 phosphorylation as compared to the documented effects of PGE_2 (Figure 8A). Cell lysates were harvested at the time points determined to be optimal for each protein of interest. Normal HLFs were pretreated with pirfenidone at a dose of 1 mM, selected based on pilot studies (data not shown) and previously published literature in lung fibroblasts (56). This dose abrogated TGFβ-

induced upregulation of αSMA and Col1A1 in a “prevention protocol” (Figure 8B, top panel). Notably, collagen reduction was less substantial than that of PGE_2 and was associated with hyperphosphorylation – rather than hypophosphorylation – of p38. Moreover, and in contrast to PGE_2, pirfenidone treatment of established MFs (“reversal protocol”) failed to promote their dedifferentiation, and likewise resulted in an increase in p-p38 (Figure 8B, bottom panel). Pirfenidone-induced p38 hyperphosphorylation was not associated with modulation of MKP1 protein expression (Supplemental Figure 9A).

Nintedanib was dosed at 2 μM, a dose consistent with its previously published use in vitro (67). This dose of drug markedly reduced ERK1/2 phosphorylation – a previously reported effect of nintedanib in lung fibroblasts (68) (Supplemental Figure 9B). Otherwise, the effects of nintedanib were similar to those of pirfenidone (Figure 8C). It partially prevented TGFβ-induced αSMA induction but had no effect on Col1A1 and failed to modulate p-p38. Likewise, established MFs treated with nintedanib did not demonstrate evidence of dedifferentiation or changes in p-p38. These data demonstrate that neither FDA-approved antifibrotic agent recapitulates the ability of PGE_2/MKP1 to inhibit p38 and dedifferentiate established MFs in vitro.

Discussion

The vast preponderance of existing literature concerning lung fibroblasts has focused on the molecular determinants of their activation and differentiation in an effort to identify fibrotic drivers that may be candidate targets for pharmacotherapy. While this remains an important and worthwhile strategy, far less is known about the brakes capable of promoting MF dedifferentiation and fibrosis resolution. Just as the appearance and persistence of tumor cells typically depend on the combination of oncogene activation and tumor suppressor inactivation, MF accumulation in fibrotic lungs likely involves the concomitant overactivation of drivers and the failure of critical endogenous brakes. Indeed, we have shown that the recognized tumor suppressor Krüppel-like factor 4 (KLF4) likewise serves as an antifibrotic brake in the lung which is deficient in fibrotic disease (39). Nevertheless, relatively little is known about such brakes and their capacity for promoting MF dedifferentiation, clearance, and fibrosis resolution. In this study, we established that expression of the dual-specificity phosphatase MKP1 in lung fibroblasts is critical for spontaneous fibrosis resolution following lung injury. Furthermore, we determined that MKP1 promotes MF dedifferentiation that reestablishes apoptosis sensitivity through dephosphorylation of p38α and showed that the specific p38α inhibitor VX-702 restored fibrosis resolution in fibroblast-specific MKP1 null mice. Deletion of MKP1 in fibroblasts following peak fibrosis also impeded alveolar epithelial cell regeneration, promoted parenchymal bronchiolization, and resulted in persistent inflammation, highlighting the importance of cellular crosstalk between fibroblasts and non-mesenchymal cells, as previously noted in other models of non-resolving fibrosis (69). Notably, neither of the FDA-approved antifibrotic drugs was capable of dephosphorylating p38 or promoting MF

dedifferentiation. To our knowledge this is the first study to assess the role of MKP1 in pulmonary fibrosis and the first to specifically characterize its function and regulation by pertinent mediators and pharmacologic agents within fibroblasts.

Dysregulated MAPK activity has been associated with several pathologic inflammatory and fibrotic diseases (70) including pulmonary fibrosis (25). It therefore follows that precise and timely deactivation of MAPKs in key effector cells is crucial for the restoration of tissue homeostasis following the fibrotic phase of lung injury. MKP1 is one of ten DUSP proteins that regulate MAPK signaling in a variety of mammalian cell types and tissues. The antifibrotic actions of MKP1 in lung fibroblasts in vitro (Figure 2) and its essential role in promoting fibrosis resolution in vivo (Figure 3) presented in this study further confirm the importance of MAPK regulation in pulmonary fibrosis and support the notion that MF dedifferentiation and clearance are necessary for fibrosis resolution. It is notable that both in vitro and in vivo deletion of MKP1 in lung fibroblasts was sufficient to potentiate Col1A1, FN1, and CTHRC1 expression as well as abrogate spontaneous resolution, respectively, despite the ostensibly redundant MAPK inhibitory activity of other MKP proteins. One possibility for the dominant role of MKP1 on the lung fibroblast phenotype is that other DUSP/MKP genes are expressed at relatively low levels – as suggested by publicly available single cell data (Figure 1) – and/or are not sufficiently upregulated during resolution. Alternatively, the specific regulatory niche fulfilled by each MKP may be distinct owing to differences in spatial restriction and substrate selectivity. Consistent with this possibility, and in direct contrast with the actions of MKP1 demonstrated in this work, a previous study revealed that *DUSP10*/MKP5 was crucial for TGFβ-induced SMAD3 activation in lung fibroblasts, was upregulated in IPF fibroblasts, and that its

global deletion mitigated bleomycin-induced pulmonary fibrosis (71). These findings highlight the important operative differences among these two MKP proteins. In contrast to MKP1, MKP5 lacks a nuclear localization sequence and can thus also influence MAPK activity from the cytoplasm (26). Furthermore, MKP1 and MKP5 have been shown to exhibit opposite regulatory roles in cardiac fibrosis (72) and muscle repair (30) – with MKP1 serving as an antifibrotic brake in the heart and positively regulating skeletal muscle myogenesis, respectively. The opposing actions of MKP1 and MKP5 are therefore not unprecedented and reinforce the complexity of MKPs in the regulation of cellular phenotypes. Although it remains to be determined whether MKP1 is the only dual specificity phosphatase that can dedifferentiate MFs and function as a brake on pulmonary fibrosis, our in vivo work suggests that it is the most important endogenous brake among the MKPs.

Remarkably, although MKP1 is known to interact with all three MAPKs, our data demonstrate that its overexpression in lung fibroblasts substantially dephosphorylates p38 but not ERK or JNK (Figure 4A). Importantly, deletion of MKP1 led to hyperphosphorylation of p38, suggesting that MKP1 exerts a measurable baseline inhibitory tone on p38 activation in MFs. Further investigation revealed that the p38α isoform is the predominant downstream target of MKP1 given its established inability to inhibit the p38ɣ and δ isoforms and the paucity of p38β expression within lung fibroblasts (Figure 5). Post-translational modifications to MKPs are known to influence their affinity for particular MAPK substrates (26) and thus may explain the selectivity of MKP1 for p38 in lung fibroblasts. One potential explanatory mechanism is acetylation of MKP1 at Lys59, which has been demonstrated to substantially increase its affinity for p38 (73). Regulation of protein acetylation itself is a complex process resulting from the net

effect of acetyltransferases such as p300 – known to catalyze acetylation of MKP1 at Lys59 (47) – and deacetylases (SIRT proteins) whose actions are known to influence fibroblasts in IPF (74). MKP1 may therefore exhibit different regulatory effects on MAPKs within various cell types in the lung dependent upon complex contextual inputs on its post-translational regulation.

The ability of the p38α-specific inhibitor VX-702 to restore fibrosis resolution in mouse lungs whose fibroblasts lack MKP1 (Figure 6) strongly suggests that p38α is indeed the singular p38 isoform driving persistent fibrosis and that its inhibition by MKP1 is required for spontaneous fibrosis resolution. These in vivo data are further supported by our findings that both CRISPR/Cas9-mediated deletion of p38α and the specific p38α inhibitor VX-702 led to MF dedifferentiation (Figure 5C – E) and restoration of apoptosis sensitivity in vitro (Figure 5F). The ability of VX-702 to mitigate peak fibrosis in vivo suggests that the alpha isoform also drives pulmonary fibrogenesis. Notably, p38α expression in resident cardiac fibroblasts has been shown to promote their differentiation into MFs and drive cardiac fibrosis following ischemic injury (75), suggesting that p38α exerts a general profibrotic effect in fibroblasts within various tissues. Although our data reveal that fibroblasts represent the primary cell in which inhibiting p38α is likely to account for fibrosis resolution, we cannot exclude possible contributing actions and benefits of inhibiting p38α in other cell types.

The precise timing of MKP1-mediated p38α inhibition during fibrogenesis and fibrosis resolution, as well as what endogenous mediator(s) might upregulate MKP1 expression and/or influence its interaction with p38, remain important unanswered questions. With regards to its upregulation, we found that diminished MKP1 expression was restored in MFs by day 42 – a finding associated with disorganized αSMA stress fibers and apoptosis (Supplemental Figure

3A). Additionally, given that the cAMP/PKA pathway robustly increased MKP1 expression with concomitant p38 dephosphorylation (Figure 7), we speculate that this second messenger pathway might be important for the MKP1 restoration required for MF clearance and fibrosis resolution. Indeed, PGE_2 – whose antifibrotic actions on MFs are due to cAMP/PKA (76) – required MKP1 to dephosphorylate p38 and promote MF dedifferentiation (Figure 7B and C). We have also shown that expression of the antifibrotic transcription factor KLF4 is rapidly and substantially increased through the cAMP/PKA pathway (39). Whether the antifibrotic actions of MKP1 and KLF4 depend upon distinct downstream molecular mediators or are interdependent is another important question for future studies.

The FDA-approved drugs pirfenidone and nintedanib fail to halt or reverse the inevitable decline in lung function associated with IPF, thus exposing a major unmet clinical need for therapies that can reverse fibrosis. As MKP1 expression in lung fibroblasts serves as an antifibrotic brake capable of resolving pulmonary fibrosis, pharmacotherapies that increase its expression or directly inhibit p38α, would be predicted to be beneficial. To provide further credence for this possibility, we demonstrated that neither pirfenidone nor nintedanib has the ability to dephosphorylate p38 or dedifferentiate MFs (Figure 8). Therefore MKP1-mediated inhibition of p38α appears to be mechanistically distinct from the actions of currently available antifibrotic therapies. Furthermore, despite its putative p38ɣ inhibitory effect (77), pirfenidone actually promoted total p38 phosphorylation in both a prevention and reversal context in precise contrast to the actions of PGE_2 (Figure 8B), direct adenylyl cyclase activation, or PKA activation (Figure 7A). It is intriguing that these in vitro results correlate with the apparent superior clinical benefit of a phosphodiesterase 4B inhibitor (which enhances intracellular cAMP

levels) in IPF patients compared to pirfenidone and nintedanib in a recent phase 2 clinical trial (78). The fact that both of these approved therapies exhibited a modest ability to prevent TGFβ-mediated upregulation of αSMA and Col1A1, but failed to promote MF dedifferentiation, is mechanistically consistent with their ability to slow disease progression while failing to reverse fibrosis.

Collectively, our findings identify MKP1 as a novel antifibrotic brake in lung fibroblasts, cAMP/PKA as a candidate endogenous pathway promoting MKP1 expression/activity, and p38α as the essential fibrotic driver inhibited by MKP1. Future studies will be necessary to determine the mechanism by which MKP1 expression and p38α activity within lung fibroblasts influence other cell types within the lung, their effect in non-pulmonary fibroblasts, and influence within other lung disease contexts – such as lung cancer – where MKP1 expression is altered (79). Our study provides novel insight into the molecular pathways within lung fibroblasts that promote fibrosis resolution following lung injury and thus provide potential targets for new therapies in IPF mechanistically distinct from those of pirfenidone and nintedanib.

Methods

Sex as a biological variable. Our study examined male and female animals, and similar findings are reported for both sexes.

Animal Studies. WT male and female C57BL/6 mice were obtained from Jackson Laboratories and used at 8 – 10 weeks of age. Transgenic mice containing *loxP* sites flanking exons 2 and 3 of the *Dusp1* locus were generated as previously detailed (38). These *Dusp1*$^{fl/fl}$ were crossed with *Col1a2*$^{CreERT2+/0}$ mice (Jackson Laboratories, strain #:029567) to generate tamoxifen-inducible fibroblast-specific conditional MKP1-KO mice. Genotyping was performed using genomic DNA extracted from tails. Briefly, genomic DNA was extracted using REDExtract-N-Amp Tissue PCR Kit (Millipore-Sigma). Cre genotyping was performed by qPCR using a *Col1a2*-Cre-specific primer pair (forward 5'-CAGGAGGTTTCGACTAAGTTGG-3' and reverse 5'-CATGTCCATCAGGTTCTTGC-3'). PCR primers designed to bind to exon 3 and the 3' *loxP* were used (5'-GCTGGCAGAGGTCTAGGAGG-3' and 5'-CATGAGGTAAGCAAGGCAGATG-3', respectively) to verify the homozygosity of the floxed allele for *Dusp1*. PCR primers designed to flank the *loxP* regions of the *Dusp1*^{fl} locus (forward: 5'-TCCTTCTTCGCTTTCAACGC-3' and reverse: 5'-GCCTGGCAATGAACAAACAC-3') were used to confirm successful recombination following tamoxifen administration in Cre positive mice.

For peak and resolution studies, pulmonary fibrosis was induced in mouse lungs following single-dose o.p. bleomycin administration (1.0 U/kg, Sigma-Aldrich, B5507), as described previously (39). To determine the role of MKP1 during fibrogenesis or spontaneous fibrosis

resolution, its fibroblast-specific deletion was achieved through tamoxifen-induced Cre activation. Specifically, tamoxifen chow (40 mg/mouse/day; Inotiv, TD.130859) was administered starting on days 9 or 21 to delete MKP1 during the fibrotic phase and resolution phase, respectively, and continued until harvest at indicated time points. To assess the role of p38α during fibrogenesis in WT mice or the resolution phase in mice whose fibroblasts lack MKP1, VX-702 (10 mg/kg o.g.) was administered daily starting on day 9 or 21, respectively, until sacrifice. Mice were sacrificed on days 21, 42, 56, or 63 as indicated. Lungs were perfused with cold PBS and the right upper, middle, and left lung lobes were harvested to assess fibrotic endpoints. Specifically, lung lobes were combined in PBS, homogenized, and assessed for hydroxyproline content to estimate total collagen and whole lung RNA while the right lower lobe was used to generate fibroblast cultures in vitro or sectioned to perform Masson's trichrome staining and imaged using bright-field whole slide imaging with a Vectra Polaris Brightfield Scanner.

Gain- and loss-of-function studies. MKP1 or GFP overexpressing fibroblast lines were generated by infection with lentiviral particles containing pLVX-TetOne-Puro-hDUSP1 or pLVX-TetOne-Puro-eGFP (Addgene) plasmids. Stable inducible fibroblast lines capable of CRISPR/Cas9-mediated deletion of MKP1, p38α, and p38ɣ were generated via infection with lentiviral particles containing pLentiCRISPR v2 TLCV2 plasmids (Addgene #87360) controlling the following sgRNA sequences: *DUSP1*: 5'-CGTCCAGCAACACCACGGCG-3', *MAPK14*: 5'-CACAAAAACGGGGTTACGTG-3', and *MAPK12*: 5'-CTCATGAAACATGAGAAGCT-3'. A non-targeting sequence: 5'-AAATGTGAGATCAGAGTAAT-3' (Thermo Fischer, A35526) was likewise

incorporated into TLCV2 and used as a negative control. Polybrene (2 μg/mL; Millipore-Sigma, TR-1003-G) or protamine sulfate (8 μg/mL, Sigma P4020) was added to lentiviral suspensions to enhance transduction efficiency in MRC5 and primary IPF cells, respectively, followed by puromycin selection (0.8 μg/mL) for 48 – 72 h. Conditional overexpression or CRISPR/Cas9-mediated deletion of the aforementioned genes was achieved by addition of doxycycline (1 μg/mL, Cayman Chemicals) to conditioned medium.

Statistics. Statistical analysis was performed using GraphPad Prism software version 9.1.0. Experimental data are presented as means and were analyzed for statistical significance by 1-way ANOVA with the Tukey's multiple comparisons test or paired/unpaired 2-tailed *t* test, as appropriate. $P < 0.05$ was considered significant. Error bars represent ± SEM.

Study approval. All animal experiments were carried out in accordance with the University of Michigan IACUC and conforming to the Animal Research: Reporting of In Vivo Experiments (ARRIVE) guidelines.

Data availability. Publicly available RNA-Seq data were obtained from https://cellxgene.cziscience.com/ and http://www.ipfcellatlas.com/. Values and statistics for all data points in graphs can be found in the supplemental Supporting Data Values file.

Details for remaining methods are provided in the Supplemental Methods.

Author Contributions

SMF, NW, LRP, and MPG designed the in vitro and in vivo experiments. Experiments were performed by SMF, NW, JS, JB, RLZ, and QS. Data were analyzed by SMF and NW. Transgenic mice and intellectual contributions were provided by AB. Patient-derived normal and IPF fibroblasts were provided by SKH. The manuscript was written by SMF and MPG. All authors reviewed the manuscript.

Acknowledgments

We thank members of the Peters-Golden and Huang labs for their valuable input into this work. This work was funded by the NIH grants R35 HL144979 (to MPG), K08 HL163178 (to SMF), R01 AR080152 (to AMB), R01 HL162963 (to SKH), and R35 HL160770 (to RLZ). and a Parker B. Francis Foundation fellowship award (to LRP). The graphical abstract and all Figure schematics were created with BioRender (biorender.com).

References

1. Strongman H, et al. Incidence, Prevalence, and Survival of Patients with Idiopathic Pulmonary Fibrosis in the UK. *Adv Ther.* 2018;35(5):724-36.
2. Sauleda J, et al. Idiopathic Pulmonary Fibrosis: Epidemiology, Natural History, Phenotypes. *Med Sci (Basel).* 2018;6(4).
3. Penke LR, and Peters-Golden M. Molecular determinants of mesenchymal cell activation in fibroproliferative diseases. *Cell Mol Life Sci.* 2019;76(21):4179-201.
4. Vaughan MB, et al. Transforming growth factor-beta1 promotes the morphological and functional differentiation of the myofibroblast. *Exp Cell Res.* 2000;257(1):180-9.
5. Hinz B, and Lagares D. Evasion of apoptosis by myofibroblasts: a hallmark of fibrotic diseases. *Nat Rev Rheumatol.* 2020;16(1):11-31.
6. Thannickal VJ, and Horowitz JC. Evolving concepts of apoptosis in idiopathic pulmonary fibrosis. *Proc Am Thorac Soc.* 2006;3(4):350-6.
7. Thannickal VJ. Aging, antagonistic pleiotropy and fibrotic disease. *Int J Biochem Cell Biol.* 2010;42(9):1398-400.
8. Horowitz JC, and Thannickal VJ. Mechanisms for the Resolution of Organ Fibrosis. *Physiology (Bethesda).* 2019;34(1):43-55.
9. Penke LR, et al. FOXM1 is a critical driver of lung fibroblast activation and fibrogenesis. *J Clin Invest.* 2018;128(6):2389-405.
10. Hecker L, et al. Reversible differentiation of myofibroblasts by MyoD. *Exp Cell Res.* 2011;317(13):1914-21.

11. Garrison G, et al. Reversal of myofibroblast differentiation by prostaglandin E(2). *Am J Respir Cell Mol Biol.* 2013;48(5):550-8.

12. Suzuki K, et al. Transcriptomic changes involved in the dedifferentiation of myofibroblasts derived from the lung of a patient with idiopathic pulmonary fibrosis. *Mol Med Rep.* 2020;22(2):1518-26.

13. Emelyanova L, et al. Impact of statins on cellular respiration and de-differentiation of myofibroblasts in human failing hearts. *ESC Heart Fail.* 2019;6(5):1027-40.

14. Zmajkovicova K, et al. The Antifibrotic Activity of Prostacyclin Receptor Agonism Is Mediated through Inhibition of YAP/TAZ. *Am J Respir Cell Mol Biol.* 2019;60(5):578-91.

15. Fortier SM, et al. Myofibroblast de-differentiation proceeds via distinct transcriptomic and phenotypic transitions. *JCI Insight.* 2021.

16. Braicu C, et al. A Comprehensive Review on MAPK: A Promising Therapeutic Target in Cancer. *Cancers (Basel).* 2019;11(10).

17. Kyriakis JM, and Avruch J. Mammalian MAPK signal transduction pathways activated by stress and inflammation: a 10-year update. *Physiol Rev.* 2012;92(2):689-737.

18. Yang SH, et al. MAP kinase signalling cascades and transcriptional regulation. *Gene.* 2013;513(1):1-13.

19. Marshall CJ. Specificity of receptor tyrosine kinase signaling: transient versus sustained extracellular signal-regulated kinase activation. *Cell.* 1995;80(2):179-85.

20. Keyse SM. Protein phosphatases and the regulation of mitogen-activated protein kinase signalling. *Curr Opin Cell Biol.* 2000;12(2):186-92.

21. Penke LR, et al. Prostaglandin E2 inhibits alpha-smooth muscle actin transcription during myofibroblast differentiation via distinct mechanisms of modulation of serum response factor and myocardin-related transcription factor-A. *J Biol Chem.* 2014;289(24):17151-62.

22. Yoshida K, et al. MAP kinase activation and apoptosis in lung tissues from patients with idiopathic pulmonary fibrosis. *J Pathol.* 2002;198(3):388-96.

23. Liu S, et al. FAK is required for TGFbeta-induced JNK phosphorylation in fibroblasts: implications for acquisition of a matrix-remodeling phenotype. *Mol Biol Cell.* 2007;18(6):2169-78.

24. Xiao L, et al. TGF-beta 1 induced fibroblast proliferation is mediated by the FGF-2/ERK pathway. *Front Biosci (Landmark Ed).* 2012;17(7):2667-74.

25. Kasuya Y, et al. Pathophysiological Roles of Stress-Activated Protein Kinases in Pulmonary Fibrosis. *International Journal of Molecular Sciences.* 2021;22(11):6041.

26. Caunt CJ, and Keyse SM. Dual-specificity MAP kinase phosphatases (MKPs): shaping the outcome of MAP kinase signalling. *Febs j.* 2013;280(2):489-504.

27. Theodosiou A, and Ashworth A. MAP kinase phosphatases. *Genome Biology.* 2002;3(7):reviews3009.1.

28. Lawan A, et al. Skeletal Muscle-Specific Deletion of MKP-1 Reveals a p38 MAPK/JNK/Akt Signaling Node That Regulates Obesity-Induced Insulin Resistance. *Diabetes.* 2018;67(4):624-35.

29. Bennett AM, and Lawan A. Improving Obesity and Insulin Resistance by Targeting Skeletal Muscle MKP-1. *J Cell Signal.* 2020;1(4):160-8.

30. Shi H, et al. Mice lacking MKP-1 and MKP-5 Reveal Hierarchical Regulation of Regenerative Myogenesis. *J Stem Cell Regen Biol.* 2015;1(1):1-7.

31. Mahalingam CD, et al. Mitogen-activated protein kinase phosphatase 1 regulates bone mass, osteoblast gene expression, and responsiveness to parathyroid hormone. *J Endocrinol.* 2011;211(2):145-56.

32. Jeanneteau F, and Deinhardt K. Fine-tuning MAPK signaling in the brain: The role of MKP-1. *Commun Integr Biol.* 2011;4(3):281-3.

33. Penke LRK, et al. Bortezomib Inhibits Lung Fibrosis and Fibroblast Activation Without Proteasome Inhibition. *Am J Respir Cell Mol Biol.* 2021.

34. Brondello JM, et al. The dual specificity mitogen-activated protein kinase phosphatase-1 and -2 are induced by the p42/p44MAPK cascade. *J Biol Chem.* 1997;272(2):1368-76.

35. Bhalla US, et al. MAP kinase phosphatase as a locus of flexibility in a mitogen-activated protein kinase signaling network. *Science.* 2002;297(5583):1018-23.

36. Nunes-Xavier CE, et al. Differential up-regulation of MAP kinase phosphatases MKP3/DUSP6 and DUSP5 by Ets2 and c-Jun converge in the control of the growth arrest versus proliferation response of MCF-7 breast cancer cells to phorbol ester. *J Biol Chem.* 2010;285(34):26417-30.

37. Khalil N, and Greenberg AH. The role of TGF-beta in pulmonary fibrosis. *Ciba Found Symp.* 1991;157:194-207; discussion -11.

38. Lawan A, et al. Hepatic mitogen-activated protein kinase phosphatase 1 selectively regulates glucose metabolism and energy homeostasis. *Mol Cell Biol.* 2015;35(1):26-40.

39. Penke LRK, et al. KLF4 is a therapeutically tractable brake on fibroblast activation which promotes resolution of pulmonary fibrosis. *JCI Insight.* 2022.

40. Redente EF, et al. Loss of Fas-signaling in fibroblasts impairs homeostatic fibrosis resolution and promotes persistent pulmonary fibrosis. *JCI Insight.* 2020.

41. Hecker L, et al. Reversal of persistent fibrosis in aging by targeting Nox4-Nrf2 redox imbalance. *Sci Transl Med.* 2014;6(231):231ra47.

42. Caporarello N, et al. Vascular dysfunction in aged mice contributes to persistent lung fibrosis. *Aging Cell.* 2020:e13196.

43. Tsukui T, et al. Collagen-producing lung cell atlas identifies multiple subsets with distinct localization and relevance to fibrosis. *Nat Commun.* 2020;11(1):1920.

44. Xie T, et al. Single-Cell Deconvolution of Fibroblast Heterogeneity in Mouse Pulmonary Fibrosis. *Cell Rep.* 2018;22(13):3625-40.

45. Farooq A, and Zhou MM. Structure and regulation of MAPK phosphatases. *Cell Signal.* 2004;16(7):769-79.

46. Owens DM, and Keyse SM. Differential regulation of MAP kinase signalling by dual-specificity protein phosphatases. *Oncogene.* 2007;26:3203-13.

47. Cao W, et al. Acetylation of mitogen-activated protein kinase phosphatase-1 inhibits Toll-like receptor signaling. *J Exp Med.* 2008;205(6):1491-503.

48. Moosavi SM, et al. Role and regulation of MKP-1 in airway inflammation. *Respir Res.* 2017;18(1):154.

49. Cuenda A, et al. SB 203580 is a specific inhibitor of a MAP kinase homologue which is stimulated by cellular stresses and interleukin-1. *FEBS Lett.* 1995;364(2):229-33.

50. Zou X, and Blank M. Targeting p38 MAP kinase signaling in cancer through post-translational modifications. *Cancer Lett.* 2017;384:19-26.

51. Cuadrado A, and Nebreda AR. Mechanisms and functions of p38 MAPK signalling. *Biochem J.* 2010;429(3):403-17.

52. Zarubin T, and Han J. Activation and signaling of the p38 MAP kinase pathway. *Cell Res.* 2005;15(1):11-8.

53. Slack DN, et al. Distinct binding determinants for ERK2/p38alpha and JNK map kinases mediate catalytic activation and substrate selectivity of map kinase phosphatase-1. *J Biol Chem.* 2001;276(19):16491-500.

54. Damjanov N, et al. Efficacy, pharmacodynamics, and safety of VX-702, a novel p38 MAPK inhibitor, in rheumatoid arthritis: results of two randomized, double-blind, placebo-controlled clinical studies. *Arthritis Rheum.* 2009;60(5):1232-41.

55. Haak AJ, et al. Targeting GPCR Signaling for Idiopathic Pulmonary Fibrosis Therapies. *Trends Pharmacol Sci.* 2020;41(3):172-82.

56. Borok Z, et al. Augmentation of functional prostaglandin E levels on the respiratory epithelial surface by aerosol administration of prostaglandin E. *Am Rev Respir Dis.* 1991;144(5):1080-4.

57. Wilborn J, et al. Cultured lung fibroblasts isolated from patients with idiopathic pulmonary fibrosis have a diminished capacity to synthesize prostaglandin E2 and to express cyclooxygenase-2. *J Clin Invest.* 1995;95(4):1861-8.

58. Huang SK, et al. Prostaglandin E(2) induces fibroblast apoptosis by modulating multiple survival pathways. *Faseb j.* 2009;23(12):4317-26.

59. Sommer A, et al. Synergistic activation of the mkp-1 gene by protein kinase A signaling and USF, but not c-Myc. *FEBS Lett.* 2000;474(2-3):146-50.

60. Lu TC, et al. Retinoic acid utilizes CREB and USF1 in a transcriptional feed-forward loop in order to stimulate MKP1 expression in human immunodeficiency virus-infected podocytes. *Mol Cell Biol.* 2008;28(18):5785-94.

61. Seternes OM, et al. Dual-specificity MAP kinase phosphatases in health and disease. *Biochim Biophys Acta Mol Cell Res.* 2019;1866(1):124-43.

62. Raghu G, et al. An Official ATS/ERS/JRS/ALAT Clinical Practice Guideline: Treatment of Idiopathic Pulmonary Fibrosis. An Update of the 2011 Clinical Practice Guideline. *Am J Respir Crit Care Med.* 2015;192(2):e3-19.

63. Zhang Y, et al. Histopathological and molecular analysis of idiopathic pulmonary fibrosis lungs from patients treated with pirfenidone or nintedanib. *Histopathology.* 2019;74(2):341-9.

64. Wollin L, et al. Antifibrotic and anti-inflammatory activity of the tyrosine kinase inhibitor nintedanib in experimental models of lung fibrosis. *J Pharmacol Exp Ther.* 2014;349(2):209-20.

65. Conte E, et al. Effect of pirfenidone on proliferation, TGF-β-induced myofibroblast differentiation and fibrogenic activity of primary human lung fibroblasts. *Eur J Pharm Sci.* 2014;58:13-9.

66. Tomás-Loba A, et al. p38γ is essential for cell cycle progression and liver tumorigenesis. *Nature.* 2019;568(7753):557-60.

67. Rangarajan S, et al. Novel Mechanisms for the Antifibrotic Action of Nintedanib. *Am J Respir Cell Mol Biol.* 2016;54(1):51-9.

68. Yang W, et al. Nintedanib alleviates pulmonary fibrosis in vitro and in vivo by inhibiting the FAK/ERK/S100A4 signalling pathway. *Int Immunopharmacol.* 2022;113(Pt A):109409.

69. Wang F, et al. Regulation of epithelial transitional states in murine and human pulmonary fibrosis. *J Clin Invest.* 2023;133(22).

70. Moens U, et al. The Role of Mitogen-Activated Protein Kinase-Activated Protein Kinases (MAPKAPKs) in Inflammation. *Genes (Basel).* 2013;4(2):101-33.

71. Xylourgidis N, et al. Role of dual-specificity protein phosphatase DUSP10/MKP-5 in pulmonary fibrosis. *Am J Physiol Lung Cell Mol Physiol.* 2019;317(5):L678-l89.

72. Bueno OF, et al. The dual-specificity phosphatase MKP-1 limits the cardiac hypertrophic response in vitro and in vivo. *Circ Res.* 2001;88(1):88-96.

73. Chi H, and Flavell RA. Acetylation of MKP-1 and the control of inflammation. *Sci Signal.* 2008;1(41):pe44.

74. Zeng Z, et al. Activation and overexpression of Sirt1 attenuates lung fibrosis via P300. *Biochem Biophys Res Commun.* 2017;486(4):1021-6.

75. Molkentin JD, et al. Fibroblast-Specific Genetic Manipulation of p38 Mitogen-Activated Protein Kinase In Vivo Reveals Its Central Regulatory Role in Fibrosis. *Circulation.* 2017;136(6):549-61.

76. Fortier SM, et al. Myofibroblast dedifferentiation proceeds via distinct transcriptomic and phenotypic transitions. *JCI Insight.* 2021;6(6).

77. Moran N. p38 kinase inhibitor approved for idiopathic pulmonary fibrosis. *Nat Biotechnol.* 2011;29(4):301.

78. Richeldi L, et al. Trial of a Preferential Phosphodiesterase 4B Inhibitor for Idiopathic Pulmonary Fibrosis. *New England Journal of Medicine.* 2022.

79. Wang H, et al. Interplay of MKP-1 and Nrf2 drives tumor growth and drug resistance in non-small cell lung cancer. *Aging (Albany NY).* 2019;11(23):11329-46.

A

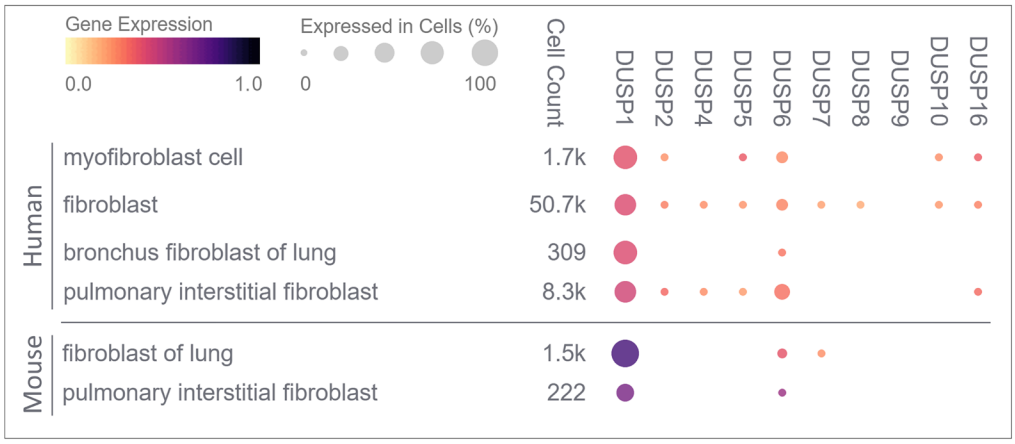
Gene Expression
0.0
1.0
Expressed in Cells (%)
0
100
Cell Count
DUSP1
DUSP2
DUSP4
DUSP5
DUSP6
DUSP7
DUSP8
DUSP9
DUSP10
DUSP16
Human
myofibroblast cell
1.7k
fibroblast
50.7k
bronchus fibroblast of lung
309
pulmonary interstitial fibroblast
8.3k
Mouse
fibroblast of lung
1.5k
pulmonary interstitial fibroblast
222

B

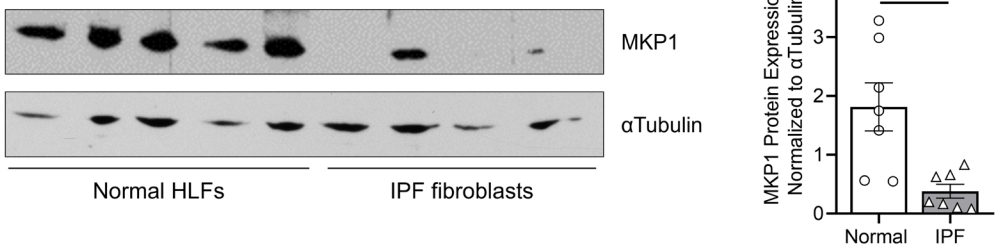
MKP1
αTubulin
Normal HLFs
IPF fibroblasts
MKP1 Protein Expression
Normalized to αTubulin
**
Normal
IPF

C

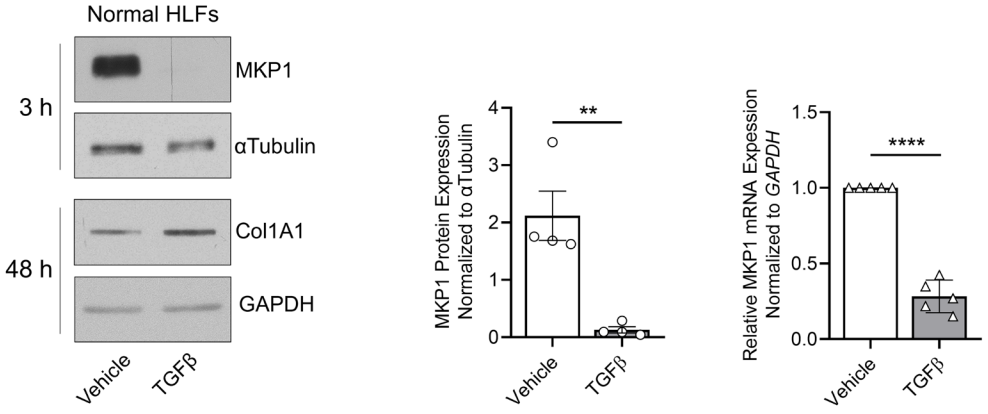
Normal HLFs
3 h
MKP1
αTubulin
48 h
Col1A1
GAPDH
Vehicle
TGFβ
MKP1 Protein Expression
Normalized to αTubulin
**
Relative MKP1 mRNA Expression
Normalized to GAPDH
****

Figure 1. MKP1 (*DUSP1*) is the chief DUSP isoform expressed in normal lung fibroblasts, is reduced in IPF fibroblasts, and is downregulated by TGFβ. (**A**) Single-cell RNA sequencing of annotated human and mouse lung fibroblast populations – generated from Chan-Zuckerberg CELL by GENE Discover online database – depicting relative expression of each catalytically active DUSP/MKP gene. Circle color denotes mean gene expression within each fibroblast subtype while circle size represents the proportion of each cell population expressing the indicated gene. (**B**) MKP1 protein expression measured by Western blot in normal and IPF patient-derived human lung fibroblasts (left: representative blot of individual patient-derived cells, right: densitometric analysis of all such cells). (**C**) MKP1 and collagen I protein expression by Western blot (left and middle) and MKP1 transcript by qPCR (right) in normal HLFs treated with TGFβ (2 ng/mL) for 3 h or 48 h as indicated in **C**. Data points represent separate experiments. Significance for densitometry data in **B** (n = 7) and **C** (n = 4) and qPCR in **C** (n = 5) was determined by 2-tailed t-test. ** $P<0.01$, **** $P<0.0001$.

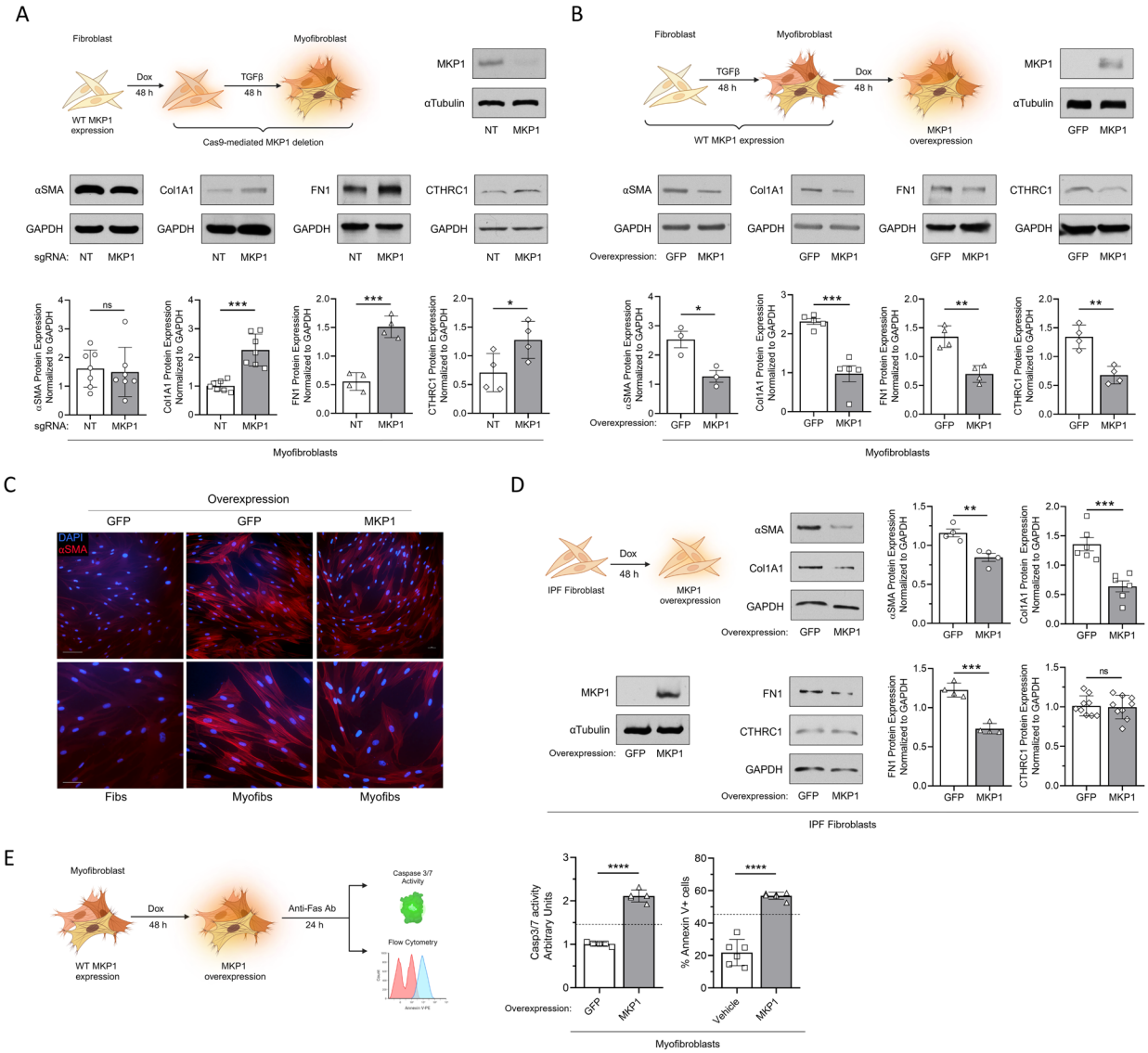
A
Fibroblast
Dox
48 h
TGFβ
48 h
Myofibroblast
WT MKP1 expression
Cas9-mediated MKP1 deletion
MKP1
αTubulin
NT
MKP1
αSMA
Col1A1
FN1
CTHRC1
GAPDH
sgRNA: NT MKP1
αSMA Protein Expression Normalized to GAPDH
Col1A1 Protein Expression Normalized to GAPDH
FN1 Protein Expression Normalized to GAPDH
CTHRC1 Protein Expression Normalized to GAPDH
ns
***
*
Myofibroblasts
B
Fibroblast
Myofibroblast
TGFβ
48 h
Dox
48 h
WT MKP1 expression
MKP1 overexpression
GFP
MKP1
Overexpression: GFP MKP1
**
Myofibroblasts
C
Overexpression
GFP
GFP
MKP1
DAPI
αSMA
Fibs
Myofibs
Myofibs
D
IPF Fibroblast
Dox
48 h
MKP1 overexpression
αSMA
Col1A1
GAPDH
MKP1
αTubulin
FN1
CTHRC1
Overexpression: GFP MKP1
IPF Fibroblasts
E
Myofibroblast
Dox
48 h
WT MKP1 expression
MKP1 overexpression
Anti-Fas Ab
24 h
Caspase 3/7 Activity
Flow Cytometry
Casp3/7 activity Arbitrary Units
% Annexin V+ cells
****
Vehicle
Myofibroblasts

Figure 2. Impact of gain- and loss-of-function of MKP1 on lung fibroblast phenotypic features. (**A**) CRISPR/Cas9-mediated *DUSP1* deletion using MKP1 or non-targeting (NT) sgRNAs in HLF-derived MFs (protocol schematic in **A**). Protein quantification by Western blot of MKP1 and the fibrosis-associated genes αSMA, Col1A1, FN1, and CTHRC1 (top: representative blot, bottom: densitometric analysis). (**B** and **C**) Inducible MKP1 overexpression in human lung MFs (protocol schematic in **B**). (**B**) Protein quantification by Western blot of MKP1 and the fibrosis-associated genes αSMA, Col1A1, FN1, and CTHRC1 (top: representative blot, bottom: densitometric analysis). (**C**) αSMA stress fibers identified by immunofluorescence microscopy using anti-αSMA-Cy3-conjugated antibody in MFs overexpressing MKP1 or GFP and fibroblast controls (using the same protocol schematic in **B**). Nuclei are stained with DAPI. Scale bars: 20 μm (top row), 10 μm (bottom row). (**D**) IPF fibroblasts harboring the same MKP1 overexpression construct as normal HLFs in (**B**), were treated with doxycycline for 48 h to induce MKP1 or GFP overexpression (protocol schematic in **D**). Protein quantification by Western blot of MKP1 and the fibrosis-associated genes αSMA, Col1A1, FN1, and CTHRC1 (left: representative blots, right: densitometric analysis). (**E**) Apoptosis sensitivity in MKP1 overexpressing (or vehicle-treated) MFs further treated with anti-Fas activating antibody (100 ng/mL) for 24 h. Apoptosis was determined by caspase 3/7 activity assay (left) or annexin V expression (right). Dashed lines represent caspase 3/7 activity or annexin V expression in untreated undifferentiated fibroblasts stimulated with anti-Fas. Sample number for each experiment "n" varied between 3 and 9 and is indicated by the number of data points in each histogram. Each blot grouping containing a protein(s) of interested and its corresponding loading control was run on a separate gel.

Significance for densitometric analysis and apoptosis activity assays determined by 2-tailed t-test. * $P<0.05$, ** $P<0.01$, *** $P<0.001$, **** $P<0.0001$.

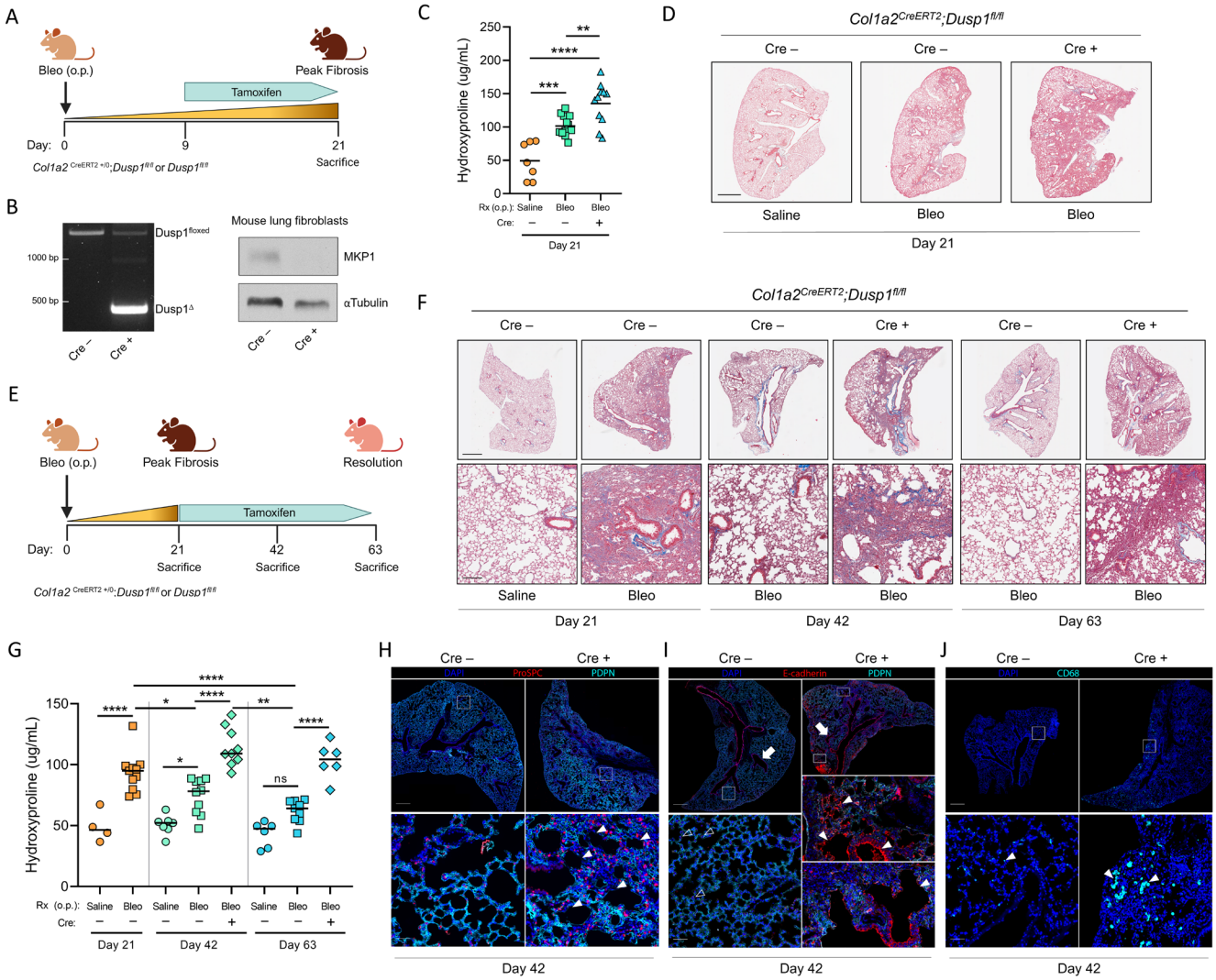
A
Bleo (o.p.)
Peak Fibrosis
Tamoxifen
Day: 0 9 21
Sacrifice
Col1a2 CreERT2 +/0;Dusp1fl/fl or Dusp1fl/fl
B
Mouse lung fibroblasts
Dusp1floxed
1000 bp
500 bp
Dusp1Δ
Cre – Cre +
MKP1
αTubulin
C
Hydroxyproline (ug/mL)
Rx (o.p.): Saline Bleo Bleo
Cre: – – +
Day 21
D
Col1a2CreERT2;Dusp1fl/fl
Cre – Cre – Cre +
Saline Bleo Bleo
Day 21
E
Bleo (o.p.) Peak Fibrosis Resolution
Tamoxifen
Day: 0 21 42 63
Sacrifice Sacrifice Sacrifice
Col1a2 CreERT2 +/0;Dusp1fl/fl or Dusp1fl/fl
F
Col1a2CreERT2;Dusp1fl/fl
Cre – Cre – Cre – Cre + Cre – Cre +
Saline Bleo Bleo Bleo Bleo Bleo
Day 21 Day 42 Day 63
G
Hydroxyproline (ug/mL)
Rx (o.p.): Saline Bleo Saline Bleo Bleo Saline Bleo Bleo
Cre: – – – – + – – +
Day 21 Day 42 Day 63
H
Cre – Cre +
DAPI PreSPC PDPN
Day 42
I
Cre – Cre +
DAPI E-cadherin PDPN
Day 42
J
Cre – Cre +
DAPI CD68
Day 42

Figure 3. Lung fibroblast expression of MKP1 mitigates peak fibrosis and is essential for spontaneous fibrosis resolution following in vivo administration of bleomycin. (**A**) Schematic illustrating the "peak fibrosis" protocol. (**B**) PCR of the *Dusp1* locus in Cre negative and positive mouse tails following tamoxifen administration (left), and subsequent MKP1 protein by Western blot in Cre negative or positive cultured lung fibroblasts (right). (**C**) Hydroxyproline content quantified from the left and right upper/middle lobe lung homogenates in saline-, Cre negative bleo-, and Cre positive bleo-treated mice at day 21. (**D**) Representative images of Masson's trichrome staining of the right lower lobe from the same mice used in **C**. Scale bar: 1 mm. (**E**) Schematic illustrating the "resolution protocol". (**F**) Representative images of Masson's trichrome staining of the right lower lobe in saline- and WT Cre negative bleo-treated mice at day 21 and saline-, Cre negative bleo-, or Cre positive bleo-treated mice on days 42 or 63. Scale bars: 1 mm (top row), 100 µm (bottom row). (**G**) Hydroxyproline content quantified from the left and right upper/middle lobe lung homogenates from the same mice used in **F**. (**H** – **J**) Immunofluorescence microscopy from bleo-treated mice at mid-resolution (day 42) depicting type I (PDPN) and type II (proSPC) alveolar epithelial cells (**H**), parenchymal bronchiolization (E-cadherin) (**I**), and alveolar macrophages (CD68) (**J**). White arrows in **I** depict normal airways. Open white arrow heads depict E-cadherin staining of type II alveolar epithelial cells. Solid white arrowheads point to alveolar regions devoid of type I cells and type II cell hyperplasia in **H**, regions of parenchymal bronchiolization in **I**, and alveolar macrophages in **J**. Scale bars: 500 µm (top row), 50 µm (bottom row). Each data point represents an individual mouse. Significance for hydroxyproline was determined by 1-way ANOVA. * $P<0.05$, ** $P<0.01$, **** $P<0.0001$.

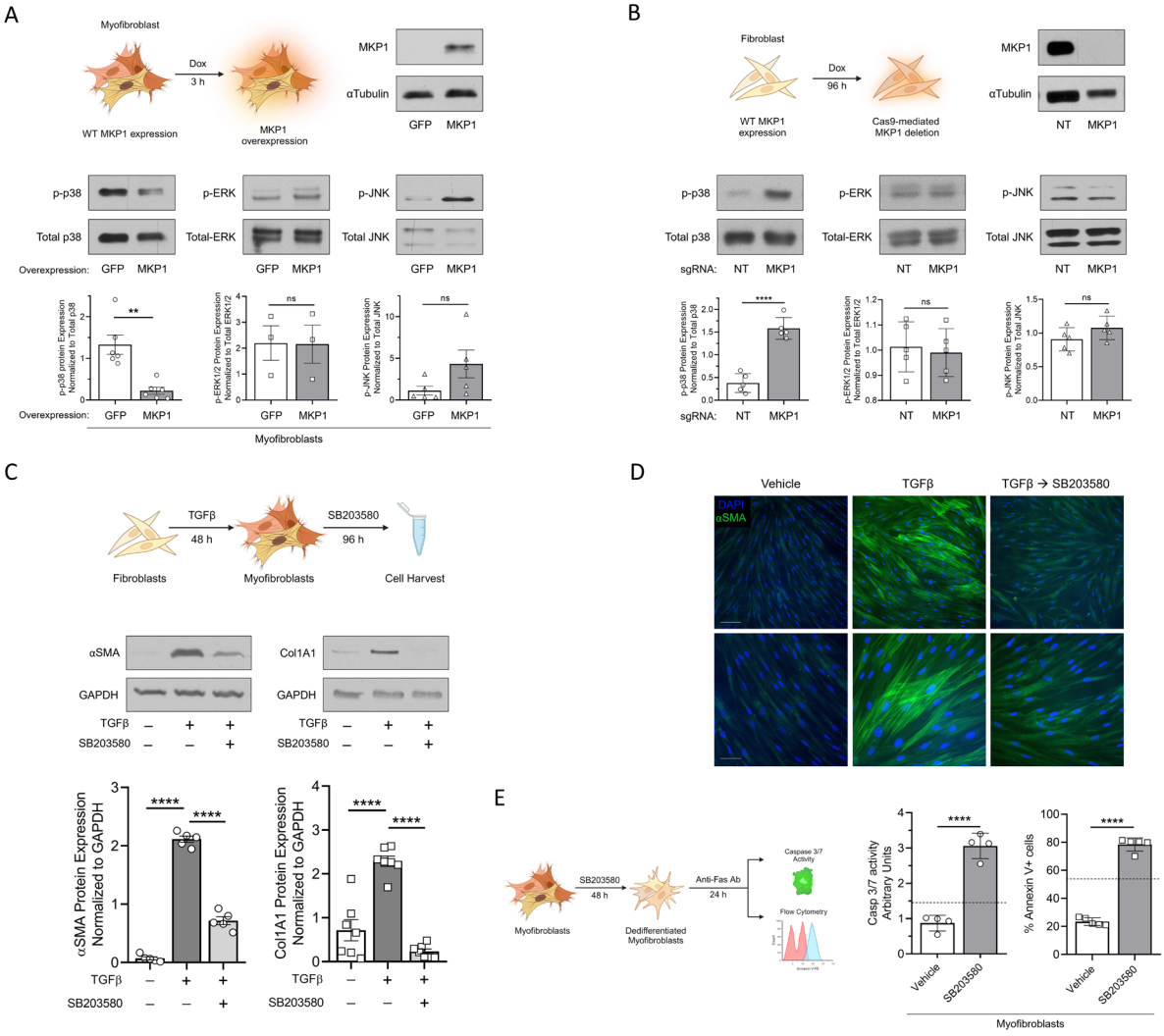
A
Myofibroblast
Dox
3 h
WT MKP1 expression
MKP1 overexpression
MKP1
αTubulin
GFP MKP1
p-p38
p-ERK
p-JNK
Total p38
Total-ERK
Total JNK
Overexpression: GFP MKP1
p-p38 protein Expression Normalized to Total p38
p-ERK1/2 Protein Expression Normalized to Total ERK1/2
p-JNK Protein Expression Normalized to Total JNK
**
ns
Myofibroblasts
B
Fibroblast
Dox
96 h
WT MKP1 expression
Cas9-mediated MKP1 deletion
NT MKP1
sgRNA: NT MKP1
****
C
TGFβ
48 h
SB203580
96 h
Fibroblasts
Myofibroblasts
Cell Harvest
αSMA
Col1A1
GAPDH
TGFβ
SB203580
αSMA Protein Expression Normalized to GAPDH
Col1A1 Protein Expression Normalized to GAPDH
D
Vehicle
TGFβ
TGFβ → SB203580
DAPI
αSMA
E
SB203580
48 h
Anti-Fas Ab
24 h
Myofibroblasts
Dedifferentiated Myofibroblasts
Caspase 3/7 Activity
Flow Cytometry
Casp 3/7 activity Arbitrary Units
% Annexin V+ cells
Vehicle
SB203580
Myofibroblasts

Figure 4. p38 is the MAPK whose inhibition by MKP1 accounts for its ability to dedifferentiate myofibroblasts. Effect of MKP1 overexpression (in MFs) or its deletion (in normal HLFs) on MAPK phosphorylation (protocol schematics in **A** and **B**). (**A** and **B**) Western blots of MKP1 and phosphorylated and total MAPK proteins (top) and densitometry analysis (bottom). (**C** and **D**) Normal HLFs were treated with TGFβ (2 ng/mL) for 48 h to generate MFs followed by treatment with the p38 inhibitor SB203580 (20 μM) for 96 h (protocol schematic in **C**; top). (**C**) Western blot analysis of the fibrosis-associated genes αSMA and Col1A1 (middle) and densitometry analysis (bottom). (**D**) αSMA stress fibers identified by immunofluorescence microscopy using anti-αSMA-FITC-conjugated antibody in MFs treated with SB203580 for 96 h and fibroblast controls (using the same protocol from the schematic in **C**). Nuclei are stained with DAPI. Scale bars: 20 μm (top row), 10 μm (bottom row). (**E**) Apoptosis sensitivity in SB203580- or vehicle-treated MFs (protocol schematic; left) via anti-Fas activating antibody (100 ng/mL) stimulation for 24 h. Apoptosis was determined by caspase 3/7 activity assay (middle) or annexin V expression (right). Dashed lines represent caspase 3/7 activity or annexin V expression in untreated undifferentiated fibroblasts treated with anti-Fas. Sample number for each experiment "n" varied between 3 and 7 and is indicated by the number of data points in each histogram. Each blot grouping containing a protein of interested and its corresponding loading control was run on a separate gel. Significance for densitometric analysis in **A** and **B** as well as apoptosis activity in **E** was determined by 2-tailed t-test while that in **C** was determined by 1-way ANOVA. ** $P<0.01$, **** $P<0.0001$.

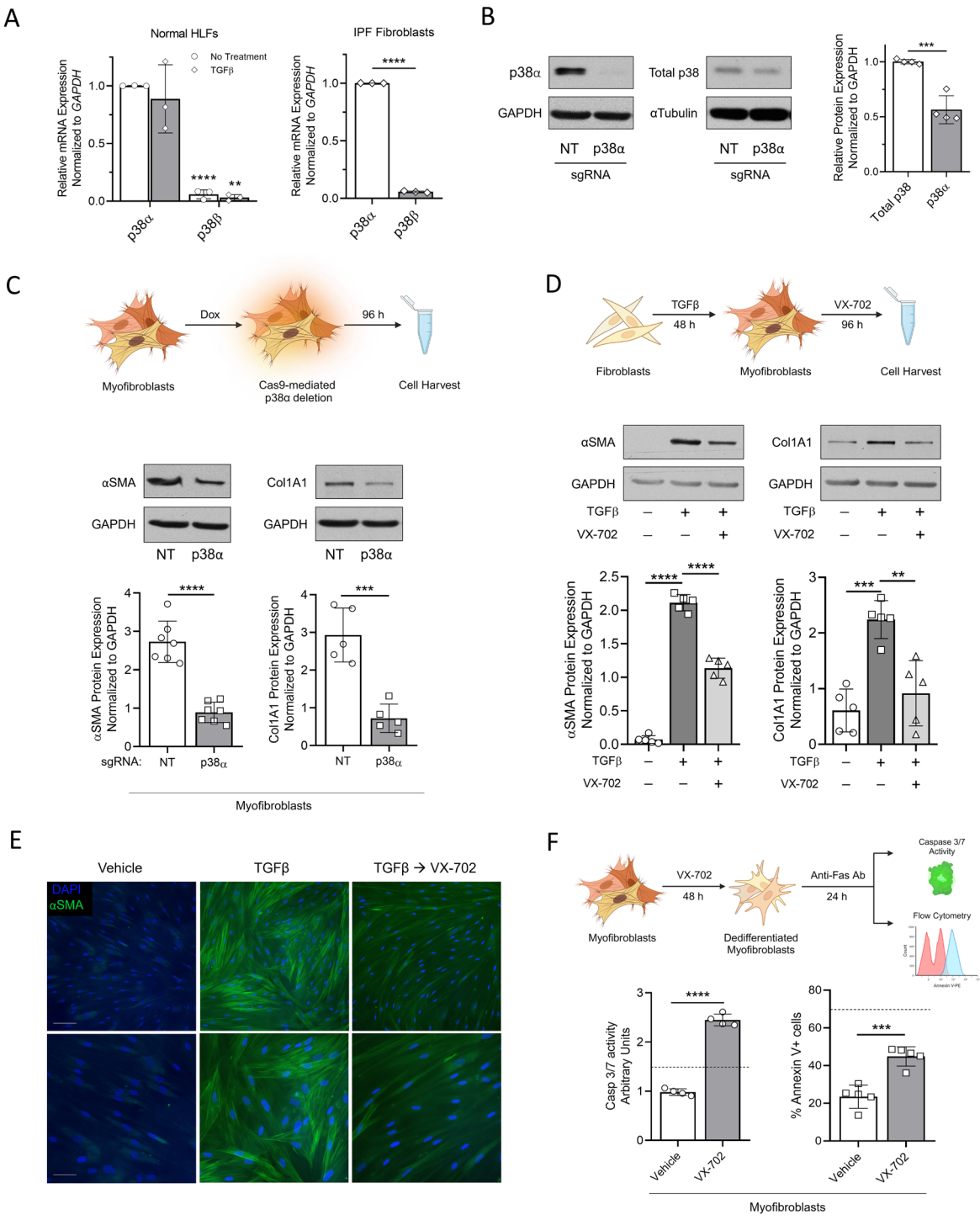
A
Normal HLFs
IPF Fibroblasts
No Treatment
TGFβ
Relative mRNA Expression Normalized to GAPDH
p38α
p38β
B
p38α
GAPDH
Total p38
αTubulin
NT p38α
sgRNA
Relative Protein Expression Normalized to GAPDH
Total p38
p38α
C
Dox
96 h
Myofibroblasts
Cas9-mediated p38α deletion
Cell Harvest
αSMA
Col1A1
αSMA Protein Expression Normalized to GAPDH
Col1A1 Protein Expression Normalized to GAPDH
sgRNA: NT p38α
Myofibroblasts
D
TGFβ
48 h
VX-702
96 h
Fibroblasts
Myofibroblasts
Cell Harvest
TGFβ
VX-702
E
Vehicle
TGFβ
TGFβ → VX-702
DAPI
αSMA
F
VX-702
48 h
Anti-Fas Ab
24 h
Caspase 3/7 Activity
Flow Cytometry
Myofibroblasts
Dedifferentiated Myofibroblasts
Casp 3/7 activity Arbitrary Units
% Annexin V+ cells
Vehicle
VX-702
Myofibroblasts

Figure 5. p38α is the isoform whose inhibition by MKP1 promotes myofibroblast dedifferentiation. (**A**) Relative p38α and β mRNA expression quantified by qPCR in normal HLFs or MFs (left) and patient-derived IPF fibroblasts (right). (**B**) Protein quantification of p38α by Western blot in normal HLFs following Cas9-mediated deletion of p38α using *MAPK14* sgRNA or non-targeting (NT) control. p38α was quantified by subtracting the densitometric value of the total p38 band in the isotype deleted line from that of the total p38 band of the WT line. (**C**) Western blot analysis of the fibrosis-associated genes αSMA and Col1A1 (middle) and densitometry analysis (bottom) following Cas9-mediated *MAPK14*/p38α deletion (protocol schematic; top). (**D** and **E**) MFs followed by treatment with the p38 inhibitor VX-702 (50 μM) for 96 h (protocol schematic in **D**; top). (**D**) Western blot analysis of αSMA and Col1A1 (middle) and densitometry analysis (bottom). (**E**) αSMA stress fibers identified by immunofluorescence microscopy using anti-αSMA-FITC-conjugated antibody. Nuclei are stained with DAPI. Scale bars: 20 μm (top row), 10 μm (bottom row). (**F**) VX-702- or vehicle-treated MFs (protocol schematic; top) treated with anti-Fas activating antibody (100 ng/mL) for 24 h. Apoptosis sensitivity was determined by caspase 3/7 activity assay (left) or annexin V expression (right). Dashed lines represent caspase 3/7 activity or annexin V expression in untreated undifferentiated fibroblasts incubated with anti-Fas. Sample number for each experiment "n" varied between 3 and 5 and is indicated by the number of data points in each histogram. Each blot grouping containing a protein of interest and its corresponding loading control was run on a separate gel. Significance for qPCR in **A**, densitometric analysis in **B,** and apoptosis activity in **F** was determined by 2-tailed t-test while the densitometric analysis in **D** was determined by 1-way ANOVA. ** $P<0.01$, *** $P<0.001$, **** $P<0.0001$.

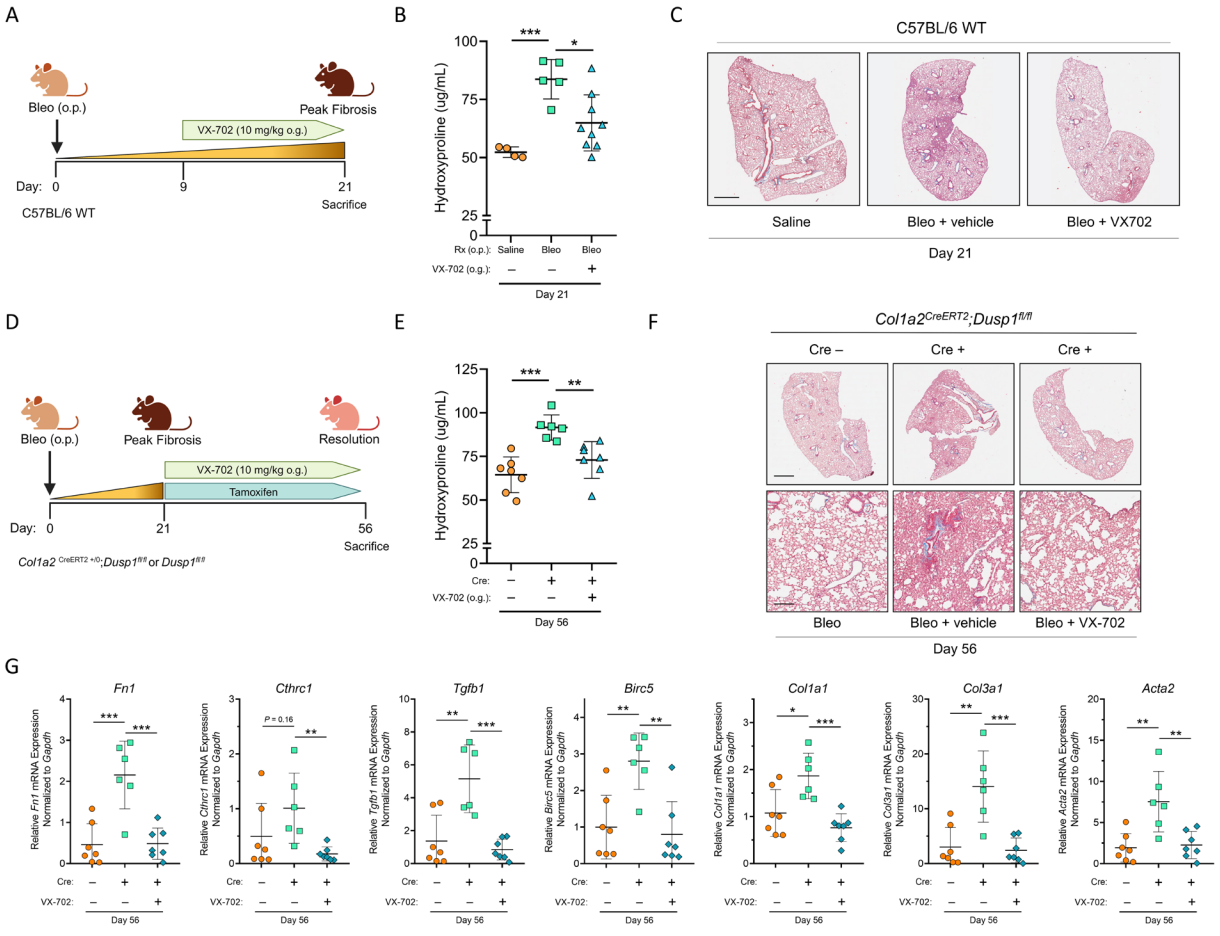
A
Bleo (o.p.)
Peak Fibrosis
VX-702 (10 mg/kg o.g.)
Day: 0
9
21
Sacrifice
C57BL/6 WT
B
Hydroxyproline (ug/mL)
Rx (o.p.): Saline Bleo Bleo
VX-702 (o.g.): – – +
Day 21
C
C57BL/6 WT
Saline
Bleo + vehicle
Bleo + VX702
Day 21
D
Bleo (o.p.)
Peak Fibrosis
Resolution
VX-702 (10 mg/kg o.g.)
Tamoxifen
Day: 0
21
56
Sacrifice
Col1a2 CreERT2 +/0;Dusp1fl/fl or Dusp1fl/fl
E
Hydroxyproline (ug/mL)
Cre: – + +
VX-702 (o.g.): – – +
Day 56
F
Col1a2CreERT2;Dusp1fl/fl
Cre –
Cre +
Cre +
Bleo
Bleo + vehicle
Bleo + VX-702
Day 56
G
Fn1
Cthrc1
P = 0.16
Tgfb1
Birc5
Col1a1
Col3a1
Acta2
Relative Fn1 mRNA Expression Normalized to Gapdh
Relative Cthrc1 mRNA Expression Normalized to Gapdh
Relative Tgfb1 mRNA Expression Normalized to Gapdh
Relative Birc5 mRNA Expression Normalized to Gapdh
Relative Col1a1 mRNA Expression Normalized to Gapdh
Relative Col3a1 mRNA Expression Normalized to Gapdh
Relative Acta2 mRNA Expression Normalized to Gapdh
Cre:
VX-702:
Day 56

Figure 6. The p38α-specific inhibitor VX-702 mitigates bleomycin induced fibrosis and restores spontaneous fibrosis resolution in mice with MKP1-deficient fibroblasts. (**A**) Schematic illustrating the "peak fibrosis" protocol. VX-702 was administered to mice daily by oral gavage (o.g.) starting day 9 through sacrifice on day 21. (**B**) Hydroxyproline content quantified from the left and right upper/middle lobe lung homogenates in saline-, bleo-, and bleo + VX-702-treated mice at day 21. (**C**) Representative images of Masson's trichrome staining of the right lower lobe from the same mice used in **B**. Scale bar: 1 mm. (**D**) Schematic illustrating the "resolution protocol". A tamoxifen chow diet was introduced and VX-702 was administered to Cre positive mice by o.g. daily starting on day 21 until sacrifice on day 56. (**E**) Hydroxyproline content (below) quantified from the left and right upper/middle lobe lung homogenates in Cre negative bleo-, Cre positive bleo-, and Cre positive bleo- + VX-702-treated mice (day 56). (**F**) Representative images of Masson's trichrome staining of the right lower lobe from the same mice used in **E**. Scale bars: 1 mm (top row), 100 μm (bottom row). (**G**) qPCR of whole lung *Fn1, Cthrc1, Tgfb1, Birc5, Col1a1, Col3a1,* and *Acta2* from the same lung homogenates used in **E**. Each data point represents an individual mouse. Significance for hydroxyproline was determined by 1-way ANOVA and for whole lung RNA by unpaired 2-tailed t-test. * $P<0.05$, ** $P<0.01$, *** $P<0.001$.

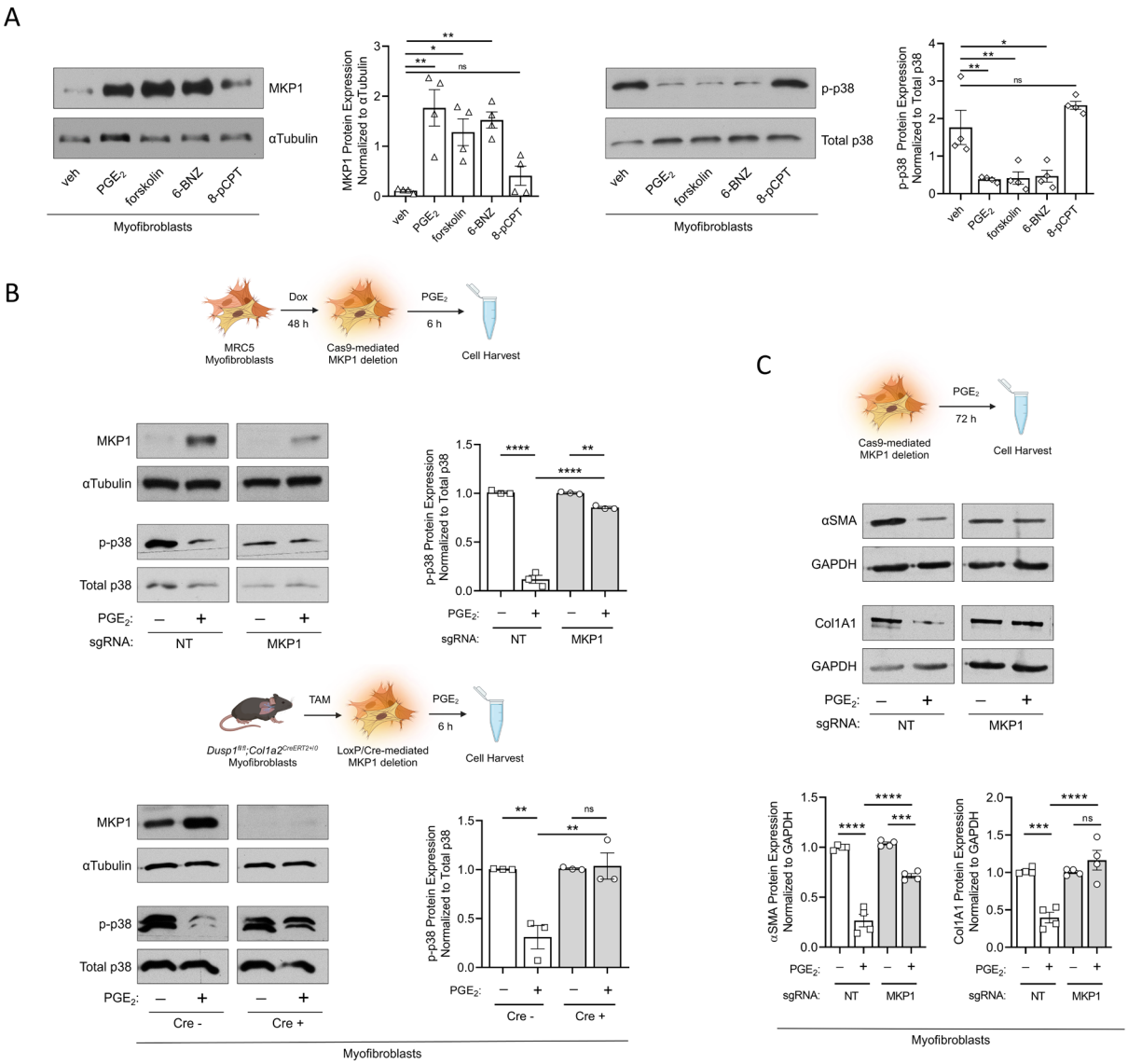
A
MKP1
αTubulin
veh
PGE2
forskolin
6-BNZ
8-pCPT
Myofibroblasts
MKP1 Protein Expression Normalized to αTubulin
p-p38
Total p38
p-p38 Protein Expression Normalized to Total p38
B
MRC5 Myofibroblasts
Dox
48 h
Cas9-mediated MKP1 deletion
PGE2
6 h
Cell Harvest
sgRNA:
NT
MKP1
Dusp1fl/fl;Col1a2CreERT2+/0 Myofibroblasts
TAM
LoxP/Cre-mediated MKP1 deletion
Cre -
Cre +
C
72 h
αSMA
GAPDH
Col1A1
αSMA Protein Expression Normalized to GAPDH
Col1A1 Protein Expression Normalized to GAPDH

Figure 7. MKP1 induction is essential for PGE_2/cAMP/PKA-mediated inhibition of p38 and myofibroblast dedifferentiation. (**A**) MKP1 and p-p38 protein quantification by Western blot in MFs treated with PGE_2 (1 μM), the direct adenylyl cyclase activator forskolin (20 μM), the PKA-specific agonist 6-BNZ-cAMP (2 mM), or the Epac-specific agonist 8-pCPT-cAMP (2 mM) for 6 h (left: representative blot, right: densitometric analysis). (**B**) MKP1, p-p38, and total p38 quantified by Western blot in doxycycline-treated lentiCRISPR HLFs containing a *DUSP1*-specific or non-targeting NT) sgRNA (top protocol schematic in **B**) or in lung fibroblasts isolated from naïve Cre positive and negative $Col1a2^{CreERT2};Dusp1^{fl/fl}$ mice (bottom protocol schematic in **B**). Human fibroblasts and mouse lung fibroblasts were subsequently treated with TGFβ (2 ng/mL – human, 5 ng/mL – mouse) for 48 h to promote the MF phenotype and then treated with PGE_2 or vehicle for 6 h, respectively (left: representative blots, right: densitometric analysis). (**C**) Protein quantification of αSMA and Col1A1 72 h following PGE_2 treatment (protocol schematic in **C**) of the same lentiCRISPR human MFs generated in **B**. Sample number for each experiment "n" varied between 3 and 4 and is indicated by the number of data points in each histogram. Each blot grouping containing a protein of interest and its corresponding loading control was run on a separate gel. Significance for densitometry analysis was determined by 1-way ANOVA. **P*<0.05, ** *P*<0.01, *** *P*<0.001, **** *P*<0.0001.

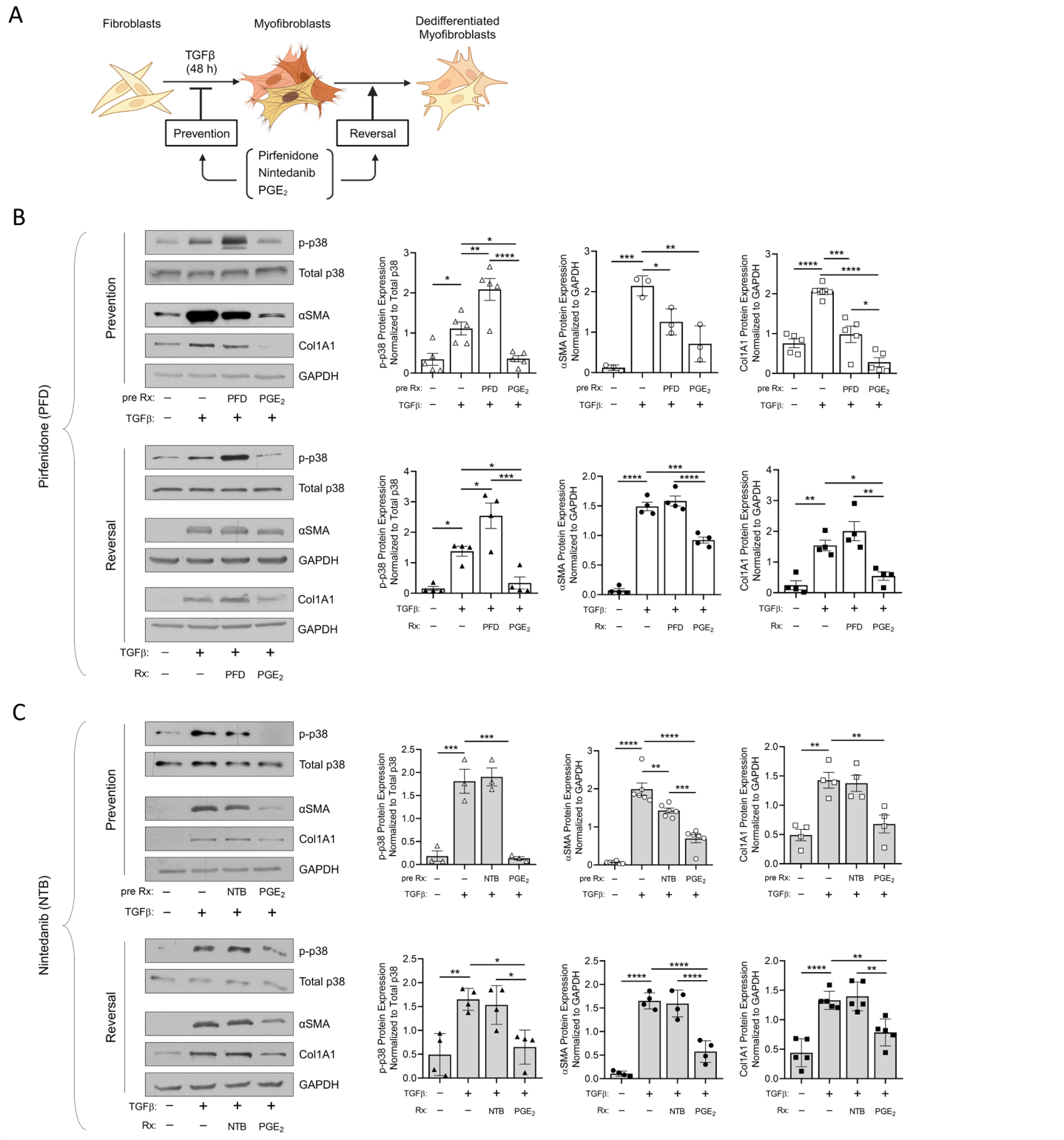
A
Fibroblasts
Myofibroblasts
Dedifferentiated Myofibroblasts
TGFβ (48 h)
Prevention
Reversal
Pirfenidone
Nintedanib
PGE2
B
Pirfenidone (PFD)
Prevention
Reversal
p-p38
Total p38
αSMA
Col1A1
GAPDH
pre Rx:
TGFβ:
Rx:
PFD
PGE2
p-p38 Protein Expression Normalized to Total p38
αSMA Protein Expression Normalized to GAPDH
Col1A1 Protein Expression Normalized to GAPDH
C
Nintedanib (NTB)
NTB

Figure 8. The two FDA approved antifibrotic drugs pirfenidone and nintedanib fail to dephosphorylate p38 and to promote dedifferentiation of human lung myofibroblasts. (**A**) Schematic illustrating in vitro MF "prevention" and MF "reversal" treatment protocols. Treatment with the antifibrotic agents pirfenidone (1 mM), nintedanib (2 μM), or the lipid mediator PGE_2 (1 μM) was administered 15 min prior to (prevention), or 48 h after (reversal) the addition of TGFβ (2 ng/mL) to culture medium. (**B** and **C**) Protein quantification of p-p38, αSMA, and Col1A1 by Western blot in normal HLFs following treatment with pirfenidone (**B**) or nintedanib (**C**) compared to PGE_2 in a prevention (top) or reversal protocol (bottom) (left: representative blot, right: densitometric analysis). For prevention studies, proteins were quantified by Western blot using cell lysates harvested at the following time points post-treatment: p-p38, 6 h; αSMA and Col1A1, 48 h. For reversal studies, proteins were quantified by Western blot using cell lysates harvested at the following time points post-treatment: p-p38, 24 h; αSMA, 72 h; and Col1A1, 48 h (**B**) or 72 h (**C**). Sample number for each experiment "n" varied between 3 and 6 and is indicated by the number of data points in each histogram. Each blot grouping containing a protein(s) of interest and its corresponding loading control was run on a separate gel. Significance for densitometric analysis were determined by 1-way ANOVA. * $P<0.05$, ** $P<0.01$, *** $P<0.001$, **** $P<0.0001$.